

Wolf-Rayet Colliding Wind Binaries

Ryan M.T. White^{a,b} and Peter Tuthill^c

^aSchool of Mathematical and Physical Sciences, Macquarie University, N.S.W. 2109, Australia

^bSchool of Mathematics and Physics, The University of Queensland, St Lucia, QLD, 4072, Australia

^cSydney Institute for Astronomy, School of Physics, The University of Sydney, N.S.W. 2006, Australia

© 20xx Elsevier Ltd. All rights reserved.

Chapter Article tagline: update of previous edition, reprint.

Glossary

Central engine refers to the binary stars at the heart of a colliding wind binary

Colliding wind nebulae are dust structures created by shocked winds of two stars, forming a spiral wrapped by the orbital motion of the stars. These are sometimes referred to as **pinwheel nebulae**.

Eddington limit is the point at which the radiation pressure from a luminous source cancels out the radially inwards gravitational attraction.

Hydrogen envelope refers to the outermost hydrogen shell of a star, where beneath this are heavier elements such as helium, carbon, etc.

Wind collision region refers to the turbulent bow shock structure where the winds of two stars are directly colliding.

Nomenclature

BSG	Blue Supergiant (star)
CWB	Colliding Wind Binary
GRB/LGRB	Gamma Ray Burst and Long GRB respectively
JWST	James Webb Space Telescope
LBV	Luminous Blue Variable (star)
OB	O or B type star
RSG	Red Supergiant (star)
SN/SNe	Supernova and Supernovae (plural form) respectively
VLT	Very Large Telescope
WC/N/O	Wolf-Rayet star of Carbon, Nitrogen, or Oxygen type respectively
WCR	Wind Collision Region
WNh	WN star with hydrogen spectra
WR	Wolf-Rayet (star)

Abstract

Wolf-Rayet stars embody the final stable phase of the most massive stars immediately before their evolution is terminated in a supernova explosion. They are responsible for some of the most extreme and energetic phenomena in stellar physics, driving fast and dense stellar winds that are powered by extraordinarily high mass-loss rates arising from their near Eddington limit luminosity. When found in binary systems comprised of two hot wind-driving components, a colliding wind binary (CWB) is formed, manifesting dramatic observational signatures from the radio to X-rays. Among the wealth of rare and exotic phenomenology associated with CWBs, perhaps the most unexpected is the production of copious amounts of warm dust. A necessary condition seems to be one binary component being a carbon-rich WR star – providing favorable chemistry for dust nucleation from the wind – however a detailed understanding of the physics underlying this phenomenon has not been established.

Key Points

- The winds of each star in binary systems collide to form bow shocks. These shocks encode the physics of each stellar wind, and are visible across the electromagnetic spectrum through both thermal and non-thermal emission.
- The systems hosting a Wolf-Rayet star are the sites of the most extreme colliding wind binaries; these Wolf-Rayet stars typically have orders of magnitude higher mass loss rates which affect the wind-wind shock physics.
- Some Wolf-Rayet colliding wind binaries – where the conditions at the shock are just right – are prolific dust producers. This dust traces the orbital motion of the shock with the binary stars, presenting itself as spiral nebulae that are bright in the infrared.
- The observational characteristics of the Wolf-Rayet colliding wind binaries are tied to orbital phase, and can result in transient peaks in X-ray/infrared/radio emission. Continued monitoring of these systems reveals their orbits, wind physics, and stellar parameters.
- Modelling of these systems is undertaken in a variety of ways depending on the wavelength regime and type of data. Photometric, spectroscopic, hydrodynamical, and geometric modelling are all commonly used to investigate colliding wind binaries and the Wolf-Rayet and massive stars at their heart.

1 Introduction

The understanding of massive stars in our Galaxy is foundational to our understanding of the wider Universe. Massive stars are born from the densest regions within clouds of molecular gas and begin shaping their environment and their galaxy from the outset. These stars evolve very quickly – on the order of a few to tens of millions of years – and produce an abundance of metals as they do so. As they live, massive stars eject material into the interstellar medium through their strong stellar winds and through episodic eruptions. As they die, massive stars enrich the chemical content of their galaxy through powerful supernova explosions. These two processes from massive stars, stellar mass loss and supernovae, are responsible for a large fraction of the metal content in the Universe and in particular they dominate production at early epochs. For example Wolf-Rayet (WR) stage of stellar evolution contributes the majority of early carbon, nitrogen, and oxygen without which our Solar System and life as we know it could not have formed.

These Wolf-Rayet stars embody the rare and extreme end-of-life phases of the most massive stars that have shed their hydrogen envelopes through binary interactions and/or the strongest known stellar winds. Despite their intrinsic rarity – only 1 in every billion stars within the Galaxy are of WR-type – these stars exert a profound influence on the Milky Way, for example in their role as progenitors of the most energetic core-collapse supernovae: Type Ic supernova. These supernovae have been associated with long duration gamma-ray bursts: events so luminous that they are visible across the observable universe. Galactic gamma ray bursts are thought to be rare – a fortuitous outcome for life on Earth as a the impacts from an event unluckily beamed along our line of sight could be significant. Exactly how WR stars in the local Universe may produce a gamma-ray burst is yet to be conclusively understood as the mechanism should be disfavoured by higher metallicity at contemporary epochs. It is hypothesised that binary interactions may play a key role, imparting or preserving angular momentum of the progenitor WR star sufficient to break spherical symmetry of the supernova, enabling the gamma ray burst to take place. Since a majority of massive stars are formed in binary or multiple systems, WR binaries are therefore of particular interest.

With no confirmed direct in-situ observations of a Wolf-Rayet precursor undergoing a supernova explosion yet recorded, the current population of WR stars must be closely studied to advance our understanding of the final moments of massive stars. Of particular interest are the colliding wind binaries (CWBs) that host WR stars. When a WR star and a sufficiently massive companion are in a binary system, a wind collision region (WCR) is formed yielding observational signatures that can include non-thermal radio emission from the shock, and in rare instances, the formation of carbon-rich dust nucleated in association with the collision interface between the components' stellar winds. Such dust can be bright in the infrared streaming into circumstellar structures inflated by the stellar wind. These dusty nebulae carry structural elements engraved by the orbital motion of the colliding-wind binary itself, forming an intricate spiral structure encoding a wealth of key astrophysical quantities. For the simplest case when the orbital plane lies close to the plane of the sky, the dust nebula forms an Archimedean spiral, or a so-called 'pinwheel nebula' as a simple consequence of a rotating insertion (orbit) of matter (dust) into a spherically expanding outflow (wind). This spiral structure is sensitive to the orbital and wind parameters of both system components, encoding the underlying physics of the CWB, and by extension the properties of the hot stars that comprise the engine driving the system.

2 Origins and Basic Properties

2.1 Formation of Wolf-Rayet stars

Massive stars – for this discussion those of order 10 to $100M_{\odot}$ – form in giant molecular clouds along with their lower mass brethren (de Wit et al., 2005; Tan et al., 2014). The initial masses of stars formed within these molecular clouds follow an initial mass function (IMF) such that low mass stars are formed in much higher number than high mass stars (Miller and Scalo, 1979; Kroupa, 2001). Despite their intrinsic rarity, massive stars' vastly greater intrinsic energy output, both in the form of luminosity and high momentum winds, results in them being the dominant force in shaping their parent molecular clouds once star formation begins (Motte et al., 2018). The profound impacts even extend to galactic scales, influencing the appearance of their host galaxy (Cameron et al., 2024), for example ionising the gas in HII regions. Because massive stars naturally form in the densest central regions of molecular clouds (and in addition to their correspondingly higher gravitational influence), there is a strong preference for binarity/multiplicity in massive star systems, and with companion stars also tending towards comparably high masses (Sana and Evans, 2011; Sana, 2017; Offner et al., 2023).

A few million years after their birth, the hydrogen in the convective cores of very massive stars can be exhausted so that the star leaves the main sequence, forming heavier elements via the triple- α process (Salpeter, 1952; Woosley et al., 2002; Carroll and Ostlie, 2017). During a phase of core/shell helium or carbon-oxygen burning, the stars then usually evolve into supergiant stars. Depending on the initial mass of the star, this could mean a red or blue supergiant (RSG and BSG respectively), or a luminous blue variable (LBV) star for the more massive stars (Groh et al., 2013). Whether through one or a combination of mass loss mechanisms such as stellar winds and/or binary mass transfer, the highest mass ($\geq 20M_{\odot}$) stars shed their outer hydrogen envelopes leaving an exposed helium star or Wolf-Rayet star (WR; Paczyński, 1967; Conti, 1975; Crowther, 2007). The exact progression of envelope/mass loss is a topic of active research, and depends very sensitively on the mass, metallicity, and rotation of the star among other variables (Meynet et al., 2011; Sander and Vink, 2020; Josiek et al., 2024); the most massive stars ($> 25M_{\odot}$) may skip the supergiant phase altogether and evolve off the main sequence directly into a WR star (Crowther, 2007; Groh et al., 2013).

2.2 The Wolf-Rayet Spectrum and Stellar Wind

Wolf-Rayet stars are characterised by extremely strong, dense stellar winds driven by emission lines of helium, carbon, nitrogen, and/or oxygen (Wolf and Rayet, 1867; Hamann et al., 2006; Crowther, 2007, and Figure 1). Despite the hydrogen envelope shedding and high

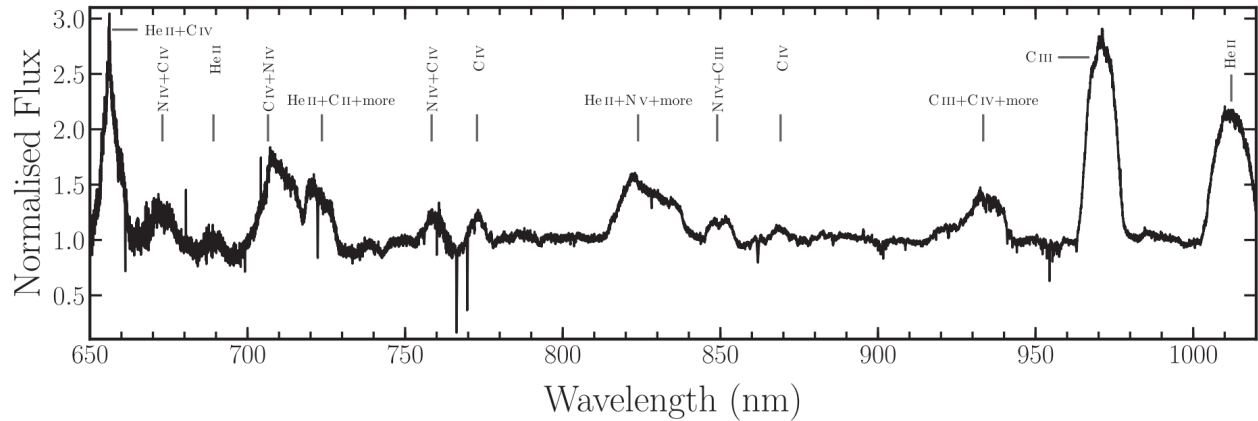


Fig. 1 The spectrum of the WR+WR system Apep shows emission lines of both WC and WN Wolf-Rayet species (Callingham et al., 2020). In particular, the WC star is mainly identified through C III and C IV lines while the WN star through the He II and N lines.

mass loss rates, WRs remain very massive at $\geq 10M_{\odot}$, depending on their spectral type. Within the Wolf-Rayet classification, there are 3 main subclassifications labelled for carbon, nitrogen, and oxygen: the WN type (owing to strong He and N lines), the WC type (owing to an absence of N and prominence of C), and the WO type (an absence of N and strong presence of O) (Gamow, 1943; Crowther, 2007). Within each of these subclassifications there exist subtypes that describe the relative strength of individual emission lines (WN2-11, WC4-9, and WO1-4) and hence more specific chemical and physical properties of the stars. The relationship between the different classes of WR stars has long been understood to be an evolutionary progression from one type to another (depending on the initial mass of the star; Conti, 1975; Abbott and Conti, 1987), although this has been recently challenged (McClelland and Eldridge, 2016, suggesting that the subtype is mass-dependent) indicating that even the fundamental properties of these stars are still a topic of active research.

In the last 30 years, there has been interest in a peculiar class of WR star: the WNh type. Wolf-Rayet stars of the WNh subclassification are categorically disparate from the classical WRs of C/N/O type; while they do display strong helium and nitrogen spectral lines characteristic of WN stars, they also exhibit hydrogen lines (hence the appended “h”) which suggests either a transitory stage of evolution or a different phenomenology altogether (Shenar, 2024). The 60 – 100 M_{\odot} mass of these stars – a factor of a few higher than typical WC/WN stars – cements these as massive stars still undergoing core-hydrogen burning, although perhaps near the terminal-age main sequence (de Koter et al., 1997; Smith and Conti, 2008; Shenar, 2024). Still, their mass loss rates are many times higher than ordinary main sequence O stars and their winds are expected to be radiatively driven, making all but their chemistry similar to classical Wolf-Rayets at first glance.

Despite the unknowns in their evolutionary progression, there is much about the phenomenology of Wolf-Rayet stars is believed to be well established. Arguably their most noteworthy feature is their uniquely fast, dense and powerful stellar winds. The properties of these winds have been established by multiple observational probes that reveal both intrinsic (e.g. line broadening in spectra; Milne, 1926) and extrinsic (in the interaction with the WR surrounds) phenomenology.

The most robust and well established indicator of a WR’s wind velocity can be found from its spectrum. Observing individual emission lines in the spectrum of a wind-driving star can show a P Cygni profile (Figure 2), wherein the emission line, doppler broadened by the spherical expansion of the luminous wind, has an absorption feature engraved at a wavelength corresponding to resonance with atoms streaming along the line of sight towards the observer and therefore blueshifted at the wind terminal velocity. Analysis of the shape of this line profile can yield highly precise wind speeds (Willis, 1982; Crowther, 2007; Callingham et al., 2020; Williams et al., 2021). Zavala et al. (2022) also showed that by taking several spectra at different regions of a WR nebula, a three dimensional geometric model of the nebula can be produced that encodes information not only about the wind speed, but constrains wind direction too.

Interactions of the Wolf-Rayet wind with the surrounding environment, such as the creation of nebulae or cavities in parent molecular clouds, can yield strong constraints on wind physics. In addition to those from fast WR winds, such strong interactions also arise from several classes of star exhibiting high mass loss rates, with WR phenomenology comparable only to LBVs and RSGs. It is understood that this mass loss is primarily driven by the radiation pressure acting upon metallic emission lines (Castor et al., 1975; Crowther, 2007) as the WR stars themselves lie near the Eddington limit (Gräfener and Hamann, 2008; Gräfener et al., 2011). Mass loss rates for WR stars are typically of order $10^{-5}M_{\odot}\text{yr}^{-1}$ (Barlow et al., 1981; Crowther, 2007), and so this coupled with the high wind velocity means that WR winds carry exceptionally high momentum.

Over the course of the WR phase, the stellar winds of the stars can form bright nebulae (see: NGC 2359, NGC 6888, Sh 2-308) fuelled by their mass and enriched chemistry; studying the multi-epoch expansion of such nebulae delivers distances to these systems if the wind velocity is well constrained (or vice versa). One such case where nebula expansion has been observed is in the wind nebula M1-67 around WR 124 (Marchenko et al., 2010), which allowed for an independent distance estimate to the system; this has also been done with the WR PNe BD+30°3639 (Schönberner et al., 2018). As a secondary direct imaging probe of WR winds, WR stars have been observed forming cavities in the molecular material of their natal environment via ablation from their stellar winds (Baug et al., 2019, see also Dale et al., 2013 for simulations of this). This same process has been seen forming shocks when the wind interacts with the surrounding gas, sometimes

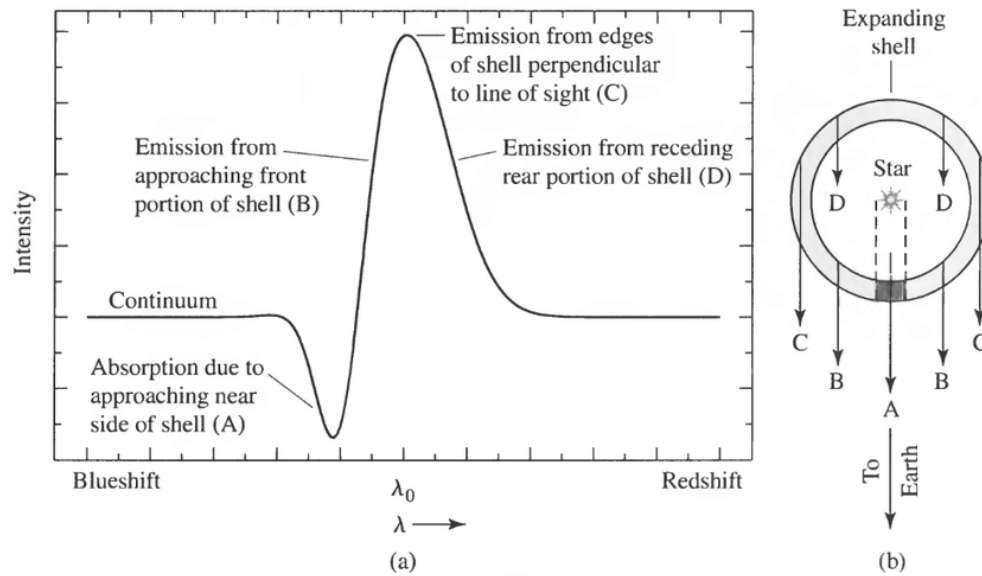


Fig. 2 Stellar spectra often show a P Cygni profile: a distinct absorption feature that is blueshifted with respect to a broader emission line [figure (a)]. This comes about due to material expanding spherically away from a central star, so that cold distant material with the highest apparent speed (directly approaching the observer) absorbs emission from interior regions, while light emitted by material streaming in other directions carries a different Doppler shift and is therefore not in resonance with the absorbing gas along the line of sight [figure (b)]. Figure from Carroll and Ostlie (2017).

triggering more star formation (Cichowolski et al., 2015).

At some scales, mass within the stellar winds is likely inhomogeneous: clumpy dust nucleation processes are believed to feature across many astrophysical theatres. Although WR stars drive mostly steady winds, there is an observed small-scale stochasticity in the winds that manifests as multi-epoch line variation (Michaux et al., 2014; Chené et al., 2020); hence, the WR stellar wind can be chemically inhomogeneous. On a related note, circumstellar dust is produced around many WR stars, especially those of WC subclassification (Allen et al., 1972; Gehrz and Hackwell, 1974; Lau et al., 2021). How delicate dust molecules are formed around WR stars – some of the hottest and most ionising astrophysical environments in existence – is still a topic of active research. The clumpy wind is one proposed avenue for dust formation, where the high opacity and density within clumps provides a sort of shielding from the environment where molecules can form (Chercheff et al., 2000). We observe orders of magnitude more efficient dust production around binary stars containing a WR, where turbulent wind compression occurs in the shocked region between the two close massive stars, providing a nurturing environment for dust creation and survival (Soullain et al., 2023).

2.3 Binaries and Colliding Winds

While it has been established that massive stars preferentially form in binary or multiple systems within the Galaxy (Offner et al., 2023), modellers also find an apparent link between the rotation rate of massive stars and their binary status. Such findings begin to fill in a broader canvas of how Wolf-Rayet stars fit within the picture of binary/multiple systems, and what this means for their evolution and observation.

Massive O stars on the main sequence are most commonly formed within binary or multiple systems, and with a predilection for companions to also be massive of O or B (sometimes abbreviated to “OB”) spectral type (Shara et al., 2022; Offner et al., 2023). Naturally, as the primary stars in these systems evolve off the main sequence into BSG/RSG or WR stars, they tend to keep their companions. Eventually, the primary star is expected to undergo a supernova explosion in which case the orbit may be disrupted causing the secondary to be ejected as a ‘runaway star’ with high velocity (typically of order the orbital velocity at the time of supernova, up to $\sim 120 \text{ km s}^{-1}$; Eldridge et al., 2011). This means that although surveys identify isolated O/B/WR stars, these may have originated within a now-disrupted binary system (Schootemeijer et al., 2024). Regardless, the Galactic WR binarity fraction is reported as $\sim 40\%$ (van der Hucht, 2001; De Marco and Izzard, 2017) with surveys of the (lower metallicity) Large and Small Magellanic Clouds (LMC and SMC, $Z \sim 0.5Z_{\odot}$ and $Z \sim 0.2Z_{\odot}$ respectively) suggest similar values. Indications are that binarity is not a strong function of either metallicity or redshift (Foellmi et al., 2003; Shenar et al., 2020; Schootemeijer et al., 2024).

Beyond the traits encompassed in the classification (two or more stars per system at least one of which is a Wolf-Rayet), the WR multiple systems seem to conform to few common rules. Companions have been found in both very close and very wide orbits, and interestingly there appears to be at least some correlation between orbital period and WR type: WN stars are more commonly found in close binaries, and WC in wide binaries (Dsilva et al., 2020, 2022, 2023). Also, while WR companions are usually similarly (or more) massive OB type stars, there are several confirmed and tentative detections of unusual companion types. Of particular note is the possible detection of a lower mass F type main sequence companion to WR 113, making the system a triple with its known WC8+O8 components (Shara et al., 2022). In the

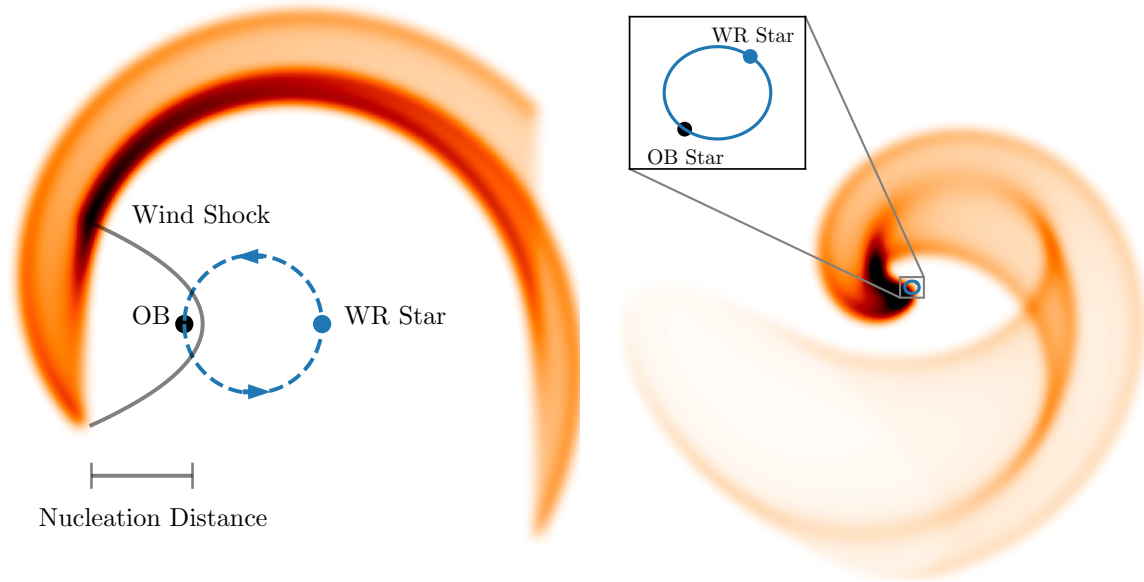


Fig. 3 *Left*: A top down view of a representative WR+OB colliding wind binary (not to scale). The WR stellar wind shocks the OB stellar wind, and dust is produced downstream (at the nucleation distance) once the shock has sufficiently cooled. As the two stars orbit (with the path defined by the dashed blue line), the produced dust nebula (nebulous orange region) wraps into a spiral. *Right*: Similar to the left plot, but inclined to $i = 30^\circ$ and at more realistic scale where the nebula is significantly larger than the orbit.

same study the authors propose a detection of a wide orbit (~ 1800 au) WN3-4 companion to the WN7 star WR 120, making it one of the few candidate WR+WR systems. Although not evolved stars, the WR 20a system has been observed to contain a WN6h+WN6h binary at its centre in an extremely short ~ 4 day orbit (Bonanos et al., 2004; Rauw et al., 2005; Olivier et al., 2022). WR 48a has been proposed as a candidate WC8+WN8h system on the basis of its spectra (Zhekov et al., 2014), although this is contested in favour of an O star companion classification (Williams et al., 2012).

Relatively recently discovered, the spectacular Apep (WR 70-16) system has been confirmed as a WC8+WN4-6 binary due to the superposition of specific spectral lines characteristic of those two classes of WR star, together with a clear wind speed discrepancy in those lines (Callingham et al., 2020). At present, Apep is the only confirmed WR+WR system composed of two evolved WR stars. The evolutionary history delivering two Wolf-Rayet stars in the same system at the same time is, like much of Wolf-Rayet evolution in general, an open question and made still more puzzling by the disparate spectral classes (WC and WN). Early studies even questioned the observability of these systems (Vrancken et al., 1991), although technique and instrumentation development has provided clear success in detection of WR binaries. With a lack of population synthesis studies showing a clear WR+WR formation channel, one possible pathway forward may lie in the study of less evolved massive stars (e.g. in the WN6h+O3/WN7 system R145; Shenar et al., 2017).

Given that Wolf-Rayet stars are known for their powerful winds and high binarity fraction, it naturally arises that we should expect some interaction phenomenology at the collision interface between the winds of the WR star and its (usually massive) companion (Cherepashchuk, 1976; Prilutskii and Usov, 1976). Indeed, there is a modest population of WR+O/B/WR binaries whose dense winds collide to produce dust nebulae that expand outwards from the system. We illustrate the diversity of such systems in Figure 7, revealing that even the same physics can produce vastly different observed nebula geometry.

3 Phenomenology

3.1 Infrared

Among the earliest infrared observations of WR stars in the 1970s uncovered increased emission particularly in the continuum to longer wavelengths, a finding known as an “infrared excess” (Allen et al., 1972; Roche and Aitken, 1984). As dust was not ordinarily expected in the hostile environs surrounding luminous hot blue stars, the infrared excesses were originally thought to arise from free-free emission (Hackwell et al., 1976). However, further observations following an infrared brightening in WR 140 revealed that the spectral energy distributions were, indeed, consistent with hot dust (Williams et al., 1978). This established WR 140 as something of a touchstone for the whole field – a status it has maintained for a half century. Because high gas densities and relatively low temperatures are considered necessary conditions for dust formation, the dust-producing WR stars posed a conundrum for astrophysics: how can copious circumstellar dust form in the immediate environment of stars with near relativistic winds, harsh UV radiation fields and extreme temperatures?

Observers found that for the latest subtypes of the WC series – classes WC7, WC8 and beyond – the presence of dust became increasingly

common, a finding attributed to the relative abundance of enriched material, particularly carbon, in the stellar wind. Addressing the riddle of the dust formation mechanism, the association of the periodic infrared brightening of WR 140 (Williams et al., 1978, 1987) with periastron passage of an eccentric binary precipitated the first major breakthrough in understanding the origins of the dust. A model emerged in which the wind collision region between the two stars was able to create and harbour a dust nursery where wind compression enhanced the density, with radiative cooling further tipping the ambient conditions in favour of nucleation (Williams et al., 1990; Usov, 1991). Wind collision region and subsequent turbulent shock provides an ample environment for dust production (Williams et al., 1990; Usov, 1991). Further mechanisms might include mixing of chemical ingredients (such as Hydrogen) at the contact discontinuity and subsequent shielding from the ionising radiation in the turbulent conical shock boundary (Hendrix et al., 2016). While details of the dust formation mechanism may remain uncertain, resulting infrared bright nebulae adorning a number of systems have generated considerable attention, yielding intricately structured forms whose geometry and periodic behaviour encode otherwise hidden orbital and wind properties of the system.

The touchstone colliding-wind binary system WR 140 is today regarded as the archetype of the episodic dust producers, while persistent dust emitter WR 104 is the prototype of the so-called ‘pinwheel nebulae’. The latter system features a circular binary orbit resulting in little intrinsic variation in the properties of the wind-wind shock and as a consequence a continuously uniform dust production rate in contrast to the orbitally-modulated IR excess for WR 140. The simplest geometry arises where the binary orbital motion lies in the plane of the sky, producing an apparent perfect spiral of dust – a structure that seems suited to the observed appearance of WR 104 (Tuthill et al., 1999). The simplest form of spiral (Archimedes, 2017, originally described by Archimedes in approx. 225 BCE) has the radial extent of a point on the curve determined purely by its outwards velocity and angular coordinate,

$$r = v \cdot \theta \quad (1)$$

Despite the simplicity of the model, for CWBs in a circular orbit constantly producing dust these Archimedean spirals have been found to trace the nebula geometry exceptionally well and dust position described by Equation 1 fits well to data from a number of systems. Where the central binary system exhibits significant ellipticity in its orbit, then the resulting spiral will deviate from the simplest family of shapes, and furthermore such systems are usually also associated with orbital modulation in the rate of dust production. Although this can manifest as a relatively smooth variation in the infrared excess with orbital phase, it more often seems to result in a ‘turn on’ and ‘turn off’ in the spiral (see Apep, WR 140 in Figure 7). Clearly this speaks to some degree of criticality in the physics of dust production, with accumulating evidence that dust production will shut off relatively quickly both under conditions where the wind shock is too weak, and where it is too strong. Such extra complexities on the geometry imposed by eccentricity and orbital modulation of dust production rate, when also coupled with the range of random inclinations that systems exhibit relative to our line of sight, results in no two colliding wind nebulae appearing the same despite the consistent and relatively simple geometry of the formation mechanism.

Although the dust nebulae produced by colliding wind binaries are orders of magnitude larger than the Solar System (see the scales in Figure 7), their Galactic distance of ≥ 1 kpc requires that high angular resolution observations are needed to resolve structure. This, coupled with the fact that the resolved dust nebulae are most luminous in the infrared, means that direct imaging of these nebulae has been a relatively recent development coevolving with high angular resolution infrared astronomy. The recovery of direct imagery of these nebulae is an essential effort as we can precisely constrain many fundamental properties of the orbit and wind that cannot be recovered by spectral or photometric analyses (see Section 3.1.2).

Most of the earliest examples of full images for these systems, such as those for WR 104 and WR 98a, were recovered with aperture masking interferometry on the Keck 1 telescope (Tuthill et al., 1999; Monnier et al., 1999; Tuthill et al., 2000). This method allowed for fully diffraction-limited observation at sufficiently high angular resolution to recover complex asymmetric structures on the characteristic scales demanded by the system architecture itself (≤ 100 mas). The intervening quarter century has seen an explosion of ground-based high angular resolution infrared astronomy, where direct images of colliding wind nebulae has become almost routine on large, 8 metre class telescopes (Marchenko et al., 2002; Marchenko and Moffat, 2007; Tuthill et al., 2008; Callingham et al., 2019, for WR 112, 48a, 104/98a, and Apep respectively), even for very distant systems near the galactic centre (Tuthill et al., 2006).

Most recent, the *James Webb Space Telescope* (JWST) has begun observing colliding wind binaries. JWST has revealed dust structures that would otherwise be difficult or impossible to obtain from ground-based facilities due to sensitivity and resolution limits imposed by the atmosphere. This has allowed observation of cooler dust at a greater distances from the central CWB engine, thereby delivering simultaneous observation of dust generated over a number of successive orbital periods taking the form of a ladder structure of nested shells (Lau et al., 2022). Not only does this allow us to determine the behaviour of dust over \sim hundreds of years (its cooling curve and lifetime, for example), this allows us to break degeneracies in our models and quantify fundamental orbital and wind parameters governing the CWB systems at very high precision.

3.1.1 Photometry and Spectra

From earliest discoveries through to contemporary studies, direct photometric and spectral observation has been the workhorse tool for understanding colliding wind binaries. Systems exhibiting episodic dust production, especially those with highly eccentric orbits, yield clear photometric signatures due to their periodic peaks in infrared brightness (e.g. for WR 137 in Figure 4). This is especially notable in systems such as WR 140 ($P \sim 7.9$ years) and WR 48a ($P \sim 32$ years) where mostly complete light curves have now been compiled since discovery (Williams et al., 1987, 2012; Peatt et al., 2023; Richardson et al., 2024). This is potentially the most efficient way to discover new CWBs: photometric monitoring can be obtained from sky survey data and only requires discrete snapshots distributed in time (perhaps even when only in the field of another target). Light curve analysis is still being used to discover new episodic dust producing CWBs (Williams, 2019) as well as being a useful tool to constrain properties such as the dust production rate when monitoring known systems.

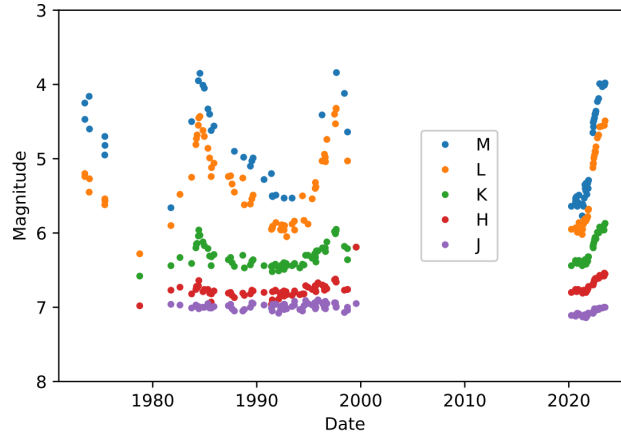


Fig. 4 The long-term infrared light curve of WR 137 shows episodic dust production in the periodic peaks. Shown here is the photometry across different infrared bands (descending band central wavelength in the legend), where the deeper infrared shows brighter total emission as a result of dust production. As the stars approach periastron every ~ 13 years, dust production turns on and eventually turns off after the stars are again sufficiently far apart. Figure from Peatt et al. (2023).

Among the earliest tools for the study of dust formation in Wolf-Rayets was the analysis of their spectra. Dust produced in these systems is relatively cool (of the order $\lesssim 1000$ K), and so has peak blackbody emission in the infrared (van der Hucht et al., 1996, for dust peaks around $10 - 15 \mu\text{m}$ in WR 48a, 98a, 104, 112, and 118). Circumstellar dust absorbs higher energy starlight, re-emitting in the infrared where the overall spectral energy density therefore indicates a luminosity far in excess of dust-free stars (Gehrz and Hackwell, 1974; Williams et al., 1978). Analysing the spectra of these systems remains a key tool in understanding their wind composition, and also their orbits (see for example the spectral decomposition of WR stars in Callingham et al., 2020).

A recent spectral analysis of a dust shell of WR 140 suggested that there exists not just one infrared peak of carbon dust emission, but two: one dust species of $T \sim 1000$ K and grain size ~ 1 nm, and another of $T \sim 500$ K and size $30 - 50$ nm (Lau et al., 2023). Further analysis showed that the ratio of these species varies in the shell number (or rather the age of the dust), and so the dust properties of any CWB are constantly evolving, not only in production, but that composition is also subject to environmental change as the shell ages.

Another promising avenue to study Wolf-Rayet stars through their spectra is in the method of spectropolarimetry. This method provides an unambiguous probe into the asphericity (or more generally anisotropy) of a stellar wind via any discrepant polarisation between continuum and line emission (Harries et al., 2000; Vink et al., 2011, see the latter for a succinct description of the method). This method has been successful in identifying wind asphericity and rapid rotation in several classes of stars, including WRs, and even in the WC+O CWB WR 137 (Harries et al., 2000; Lefèvre et al., 2005) although more recent work points to the companion not the WR star as the origin of the asymmetry (St-Louis et al., 2020). It is not unambiguously clear, at present, if this method can be made to yield a clear signal indicating stellar rotation in the environment of a WCR.

3.1.2 Hydrodynamic and Geometric Modelling

The most rigorous, although also computationally intensive, treatment of the colliding wind environment surrounding Wolf-Rayet binaries is with hydrodynamical simulations. Therein the complicated interactions of gas and dust in the environment around the binary can be simulated, offering insight into dust production and the chemical content of CWB nebulae. It is with these simulations that the dust production mechanism within CWBs was first quantified, showing that gas mixing in the turbulent shocked fluid can efficiently create dust amidst the harsh WR environment (such as in Figure 5).

These simulations are essential in predicting the geometric dust production around the shock, as well as comparing the state of theory with observations. One of the most easily observed and important parameters describing colliding wind nebulae, no matter the orientation, is the shock opening angle. The opening angle uniquely describes the momentum ratio between the two stellar winds in the binary, defined from stellar mass loss rates and wind terminal velocities as

$$\eta = \frac{\dot{M}_1 v_{\infty,1}}{\dot{M}_2 v_{\infty,2}} \quad (2)$$

for two stars of subscript 1 and 2. For a range of wind parameters, hydrodynamical simulations have accurately linked the wind momentum ratio and shock opening angle. Notably, hydrodynamical simulations were used to suggest that dust production is more efficient around the trailing edge of the shock than the leading edge (with respect to the orbital motion of the stars Lamberts et al., 2012; Hendrix et al., 2016; Soulain et al., 2023). This is observationally confirmed by the ‘azimuthal variation’ in dust production around the shock cone of WR 140 in particular (Williams et al., 2009a; Han et al., 2022).

Hydrodynamical simulations have helped show just how sensitive dust production is to system parameters, explaining in large part the diversity of colliding wind nebulae. Not only has mass loss rate, wind velocity, and wind chemical composition been shown to alter the

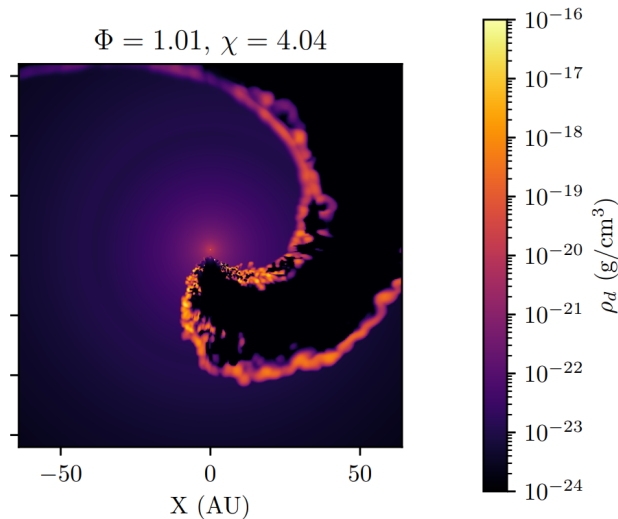


Fig. 5 Hydrodynamical simulations can accurately reproduce the conditions that result in dust production along the colliding wind shock. This figure from Eatson et al. (2022b) shows how the turbulent region in the shocked wind, here just after periastron in WR 140 where the shock cooling is adiabatic, produces large clumps of dust. The colourbar shows the dust density, ρ_d , in the region around the binary.

shock properties (Eatson et al., 2022a; Soulain et al., 2023), but even the speed of orbital motion has been suggested as a key factor in the turn on vs turn off true anomaly in eccentric systems, such as WR 140 (Eatson et al., 2022b). Further, these simulations are consistently used in the reproduction of non-thermal (primarily X-ray and radio) observations (Pittard and Dougherty, 2006; Mackey et al., 2023).

In parallel with the maturation of hydrodynamical simulations, various simple geometric models were developed to reproduce key features of colliding wind nebulae. These geometric models allow for far simpler parameter estimation of CWBs and at much faster compute time compared with hydrodynamical simulations. Archimedean spirals have been used since the first direct images of these dust nebulae (Tuthill et al., 1999), although this does not account for the volumetric geometry of the dust plume and is valid only for a narrow range of binary orbital inclinations and eccentricities. Since then, a more physically motivated geometric model has been developed which reproduces the volumetric structure of the expanding plume (shown in Figure 8). The model approximates the wind collision process by tracking rings of material that expand on the surface of a cone after encountering the nose of the wind-wind shock, expanding with a velocity corresponding to that of the radial wind. When populating a high number of rings over the orbital period, the result is a discretised expanding plume structure that faithfully emulates the true geometry of the dust nebula when interpolated. This family of geometric models was first shown in Monnier et al. (2002) for WR 140, but has since been used for Apep (Callingham et al., 2019; Han et al., 2020), WR 104 (Harries et al., 2004), WR 112 (Lau et al., 2020), WR 137 (Lau et al., 2024), and WR 140 (again, more accurately Han et al., 2022; Lau et al., 2022), with great success when compared to CWB imagery. Such a geometric model was used to show the dust nebula in Figure 3.

The wind momentum ratio (Equation 2) is a useful tool to learn about the relative properties of stellar winds in a binary. Without knowing the mass loss rates and velocities of each stellar wind – as in what we might see from a direct image snapshot of a colliding wind nebula – this is difficult to constrain, unlike the observed shock opening angle. Supported by hydrodynamical simulations, two approximate functional forms of the wind momentum ratio are commonly used. For these we need only the wind-wind shock opening angle θ_{OA} of the observed nebula. The first we state is from Eichler and Usov (1993),

$$\frac{\theta_{OA}}{2} = 2.1 \left(1 - \frac{\eta_{W/S}^{2/5}}{4} \right) \eta_{W/S}^{1/3} \quad (3)$$

which when solved – with θ_{OA} input in radians – gives information about the momentum ratio of the weaker wind (subscript W) compared to the stronger (subscript S) wind. The second equation we consider is from Tuthill et al. (2008); Gayley (2009),

$$\eta_{S/W} = \left(\frac{121}{\theta_{OA}/2} - \frac{31}{90} \right)^3 \quad (4)$$

which gives information about the stronger wind relative to the weaker wind. Both of these are approximate forms of the wind momentum ratio, but using them allows one to infer the mass loss properties of the stellar winds using simple geometric modelling only.

Somewhat similar, independent models have been published since the creation of the aforementioned geometric model. The first geometric treatment of the WCR alone was in Parkin and Pittard (2008), who modelled the shock region as a cone that rotated with orbital motion. This treatment of the geometric model involved implementing a ‘skew’ (a rotation of the WCR ring) to the WCR to account for the orbital motion of the secondary star. While this is apparently necessary to accurately model non-thermal emission from CWBs, it is not clear if this has a significant effect on dust production that would manifest in infrared imagery. An independent attempt at modelling the entire volumetric structure of the dust nebula was published in Williams et al. (2009a) for WR 140, where the resulting eccentric structure

is close to that of Monnier et al. (2002), but with added effects of dust asymmetry not unlike Han et al. (2022).

These simpler geometric models offer significant computational efficiency at a cost of physical insight. Where a hydrodynamical simulation may require runtime of hours, days, or even more, the geometric model can be evaluated on the order of seconds. This opens the door for parameter estimation using the geometric model rather than using it purely as a consistency check. As mentioned earlier, this does come at a cost of physical insight; these geometric models do not offer detailed information about dust production (e.g. dust mass, non-thermal emission, etc.), but they do offer immediate information on fundamental parameters such as orbital characteristics and dust turn on/off. As of yet, geometric models have not been used to constrain orbital parameters (eccentricity, inclination, etc.) effectively, and a proper statistical treatment with Bayesian parameter inference methods has not yet appeared in the published literature.

3.2 High-Energy Emission

Colliding wind binaries are strong X-ray sources, and were first hypothesised as such in Cherepashchuk (1976) and Prilutskii and Usov (1976). The intrinsic energetics of the colliding winds can boost these emissions to be significantly stronger than those from individual stars in isolation. Since the association of CWBs with X-ray sources, the theory modelling their properties has matured and accurately represents observations (Rauw and Nazé, 2016, for a review). Modern models reproduce X-ray spectra exceedingly well, providing insight into the mass loss rates and wind speed but also the homogeneity of the wind and its cooling physics (Zhekov, 2021; Zhekov et al., 2022). The X-ray flux of eccentric CWBs is variable as the properties at the WCR change over the course of the orbit, allowing us to constrain orbital and dust production properties; the phase of the flux peaks has been found to be wavelength dependent as the most efficient cooling mechanism at the WCR changes between radiative and adiabatic with orbital phase (Gosset and Nazé, 2016; Rauw and Nazé, 2016; Mackey et al., 2023). This kind of variation within the light curve is in conjunction with the usual eccentricity effects, as well as a WCR column density constraint on the orbital inclination in the X-ray (see Section 5.3 of Gosset and Nazé, 2016). At some inclinations, the observed X-ray emission strength may as well vary in time over the binary orbit as the nose of the wind-shock passes behind, and is partially obscured by the dense WR wind, only to rise again at a later orbital phase when traversing the thinner wind of the O star. These patterns are observed, for example, in the bright WR binary γ^2 Velorum (Stevens et al., 1995).

Given the inherent energy associated with the colliding stellar winds, we might also expect that these systems are highly luminous γ -ray emitters. Indeed, hydrodynamical modelling of colliding winds suggests that there should be a significant γ -ray emission (Huber et al., 2021; Pittard et al., 2020). Despite this, only two massive colliding wind binaries have been observed with such a γ -ray excess: η Carinae (consisting of a LBV+? binary; Reitberger et al., 2015) and γ^2 Velorum (a WC8+O7.5 system, also known as WR 11; North et al., 2007; Pshirkov, 2016). Why γ -ray emission is not abundantly visible in other CWB systems is a topic of active research. The likely reason for this lies in the WCR itself: the turbulent shocked flow is understood to be highly magnetised with a magnetic differential going from the WR side of the shock to the companion side. Grimaldo et al. (2019) find that proton acceleration in the WCR reduces this field differential and hence reduces the maximum energy of their relativistic motion, in turn hindering their eventual gamma ray emission.

The same processes that produce high energy photons in these CWBs should also accelerate electrons and protons to relativistic velocities. De Becker and Raucq (2013) share the first catalogue of CWBs that efficiently accelerate particles to such energies and briefly review the topic. The majority of the catalogue is composed of Wolf-Rayet binaries with high radio luminosities. In general, the highest energy particles accelerated in these systems will be protons, and with maximal energies of $\gtrsim 1$ TeV (Reitberger et al., 2014). The reason for this lies in the cooling mechanism at the colliding wind shock itself. As a rough measure of whether the WCR region is cooling adiabatically or radiatively, Stevens et al. (1992) introduced the cooling parameter,

$$\chi = \frac{v_8^4 d_{12}}{\dot{M}_{-7}} \quad (5)$$

which when $\ll 1$ is indicative of radiative cooling and adiabatic otherwise. Here, v_8 is the wind velocity in units of 1000 km s^{-1} , d_{12} is the star-WCR distance in units of 10^7 km , and \dot{M}_{-7} is the stellar mass loss rate in units of $10^{-7} M_{\odot} \text{ yr}^{-1}$. In the time since that paper, however, Mackey et al. (2023) have introduced an analogous parameter,

$$\chi_{\text{IC}} = \frac{1.61 v_8 d_{12}}{L_5} \quad (6)$$

which accounts for the effect of inverse-Compton cooling in the shocked wind, or cooling by additional optical line emission that briefly supplants X-ray cooling (Pollock et al., 2021). Here, L_5 is the luminosity of the star in units of $10^5 L_{\odot}$. Again, $\chi_{\text{IC}} < 1$ is evidence towards a radiatively cooling wind. Understanding whether the shocked material in the WCR is cooling radiatively or adiabatically in turn informs us of the efficiency high energy emission and particle acceleration. When the cooling is radiative, the plasma efficiently dissipates energy and free particles do not become as energetic (Reitberger et al., 2014; Rauw and Nazé, 2016). Conversely, adiabatic cooling typically results in accelerated electrons maintaining their energy. Protons are not affected by the same cooling mechanisms as electrons and in fact retain their energy within the WCR; this is why accelerated protons are more readily produced in CWBs, especially where the shock is radiatively cooling (Grimaldo et al., 2019).

3.3 Radio

Colliding wind binaries can be extremely luminous in the radio and yield a rich phenomenology amenable to study with modern facilities as well as a wealth of historical data stretching as far back as 1976 (Seaquist, 1976; De Becker and Raucq, 2013). In the radio, there are two types of physical processes that generate observed emissions. One is thermal emission due to free-free radiation in which charged particles

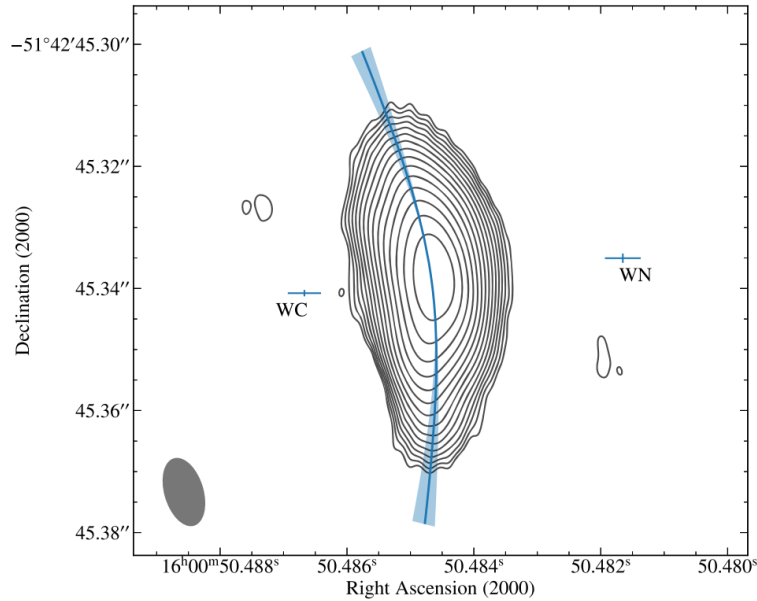


Fig. 6 The wind collision region can be directly imaged in radio wavelengths. In this figure from Marcote et al. (2021), we see the non-thermal emission at the bow shock between the two stars of the Apep system; the blue curve overlay shows the ideal shock boundary for a $\eta = 0.44 \pm 0.08$ wind collision.

(free electrons and ions) in the stellar wind rapidly accelerate under collisional electrostatic forces, emitting radiation while quickly reaching local thermal equilibrium (Wright and Barlow, 1975). The second source is non-thermal emission from synchrotron radiation, in which ultra-relativistic charged particles such as free electrons emit radiation in the radio while spiralling around magnetic field lines (Condon, 1992; Eichler and Usov, 1993; Pittard et al., 2006). These two emission mechanisms may co-exist in a single system, and even be spatially resolved at different locations as is the case of WR147, where the thermal emission is shown to originate closer to the WN star with the stronger wind, while the non-thermal emission is produced closer to the B companion (Williams et al., 1997).

The non-thermal emission from the colliding wind binaries, and its variability, can inform us of many physical phenomena at work. This non-thermal emission is particularly susceptible to absorption effects which can hinder the radio observability of these systems. Many absorption mechanisms work in parallel and to different strengths depending on the conditions at the wind collision region. Where the WCR is especially dense (for example when the two stars are close together, $\lesssim 10$ au, in their orbits), free-free absorption (Benaglia et al., 2020; Blanco et al., 2024) and synchrotron self-absorption (Kellermann, 1966; Callingham et al., 2015) work to decrease the escaped flux at low frequencies. Similarly, the Razin-Tsyvovich effect also reduces the radio flux in regions of highly magnetised material in the WCR (De Becker, 2007). All of these mechanisms together paint a picture where low energy ($\lesssim 1$ GHz) non-thermal emission is heavily modulated by the orbit of the stars, and wherein orbital progression results in strong variation for sightlines passing through the intervening ionised winds which can render them opaque to the inner WCR. Conversely, higher energy radio photons are not as affected by such absorption processes and show comparatively less modulation with the orbital phase.

Radio observations of CWBs offer information of the WCR directly, even so far as identifying the WCR itself with interferometric imaging (Dougherty et al., 2005; Rodríguez et al., 2020; Marcote et al., 2021, Figure 6). Since radio observations constrain the WCR so well, any discrepancies between wind models and data (e.g. momentum ratios, mass loss rates, etc.) are immediately apparent.

3.4 A selection of notable galactic WR CWBs

This section presents some of the most unique and significant (historically or otherwise) Wolf-Rayet colliding wind binaries for ease of reference with an emphasis on systems for which rich studies across the spectrum promise to yield a more complete picture of the astrophysics.

γ^2 Velorum As a WR+O system, itself part of a higher order 4-star system, γ^2 Velorum (WR 11) is one of the most constrained CWB orbits yet, with North et al. (2007) providing a full orbital solution from astrometry that is orders of magnitude more precise than other methods. This system is the closest and brightest WR system at merely 336^{+8}_{-7} pc (Millour et al., 2007; North et al., 2007). Despite hosting a WC8 star (De Marco and Schmutz, 1999; De Marco et al., 2000), the γ^2 Velorum system does not appreciably produce the dust that is typical of these binary configurations (van der Hucht et al., 1996). With that said, the spiral density perturbations arising from the WCR (with analogous phenomenology to the dust nebulae) have been used to explain the ‘enshrouded’ companion O star spectrum in the system (Lamberts et al., 2017).

WR 19 This system is one of the most eccentric and longest period colliding wind binaries known, with $e \approx 0.8$ and $P_{\text{orb}} = 10.1 \pm 0.1$ yr (Veen et al., 1998; Williams et al., 2009b; Williams, 2019). At present, there are no direct images of WR 19 published in the literature,

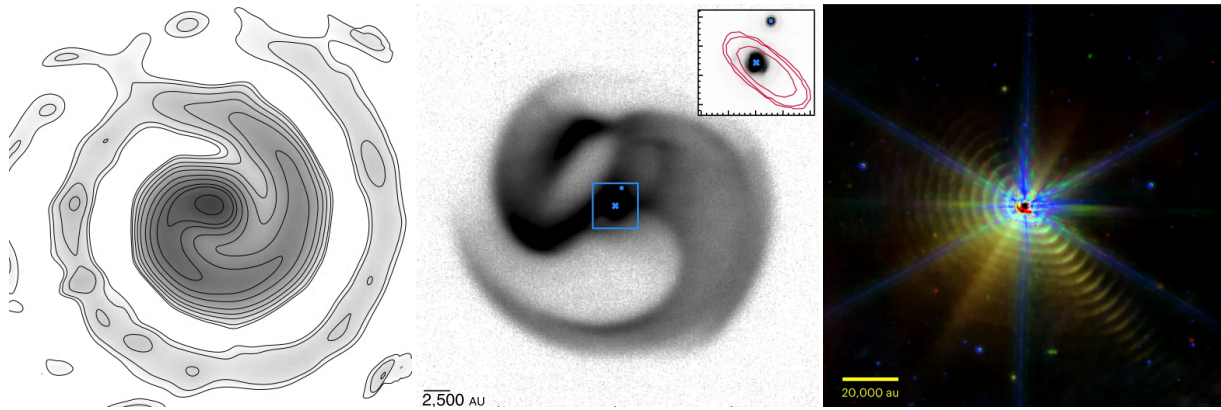


Fig. 7 The last ~ 20 years has seen much progress in imaging the dust nebula colliding wind binaries. *Left:* The first imaged CWB Pinwheel, WR 104 (Tuthill et al., 2008) recovered from interferometric data. *Centre:* The only confirmed WC+WN system in the Galaxy, Apep (Callingham et al., 2019), taken with the VISIR instrument on the Very Large Telescope (VLT). *Right:* The first CWB directly imaged with the *James Webb Space Telescope*, WR 140 (Lau et al., 2022), bears witness to more than a century of dust production in the form of ~20 concentric nested shells.

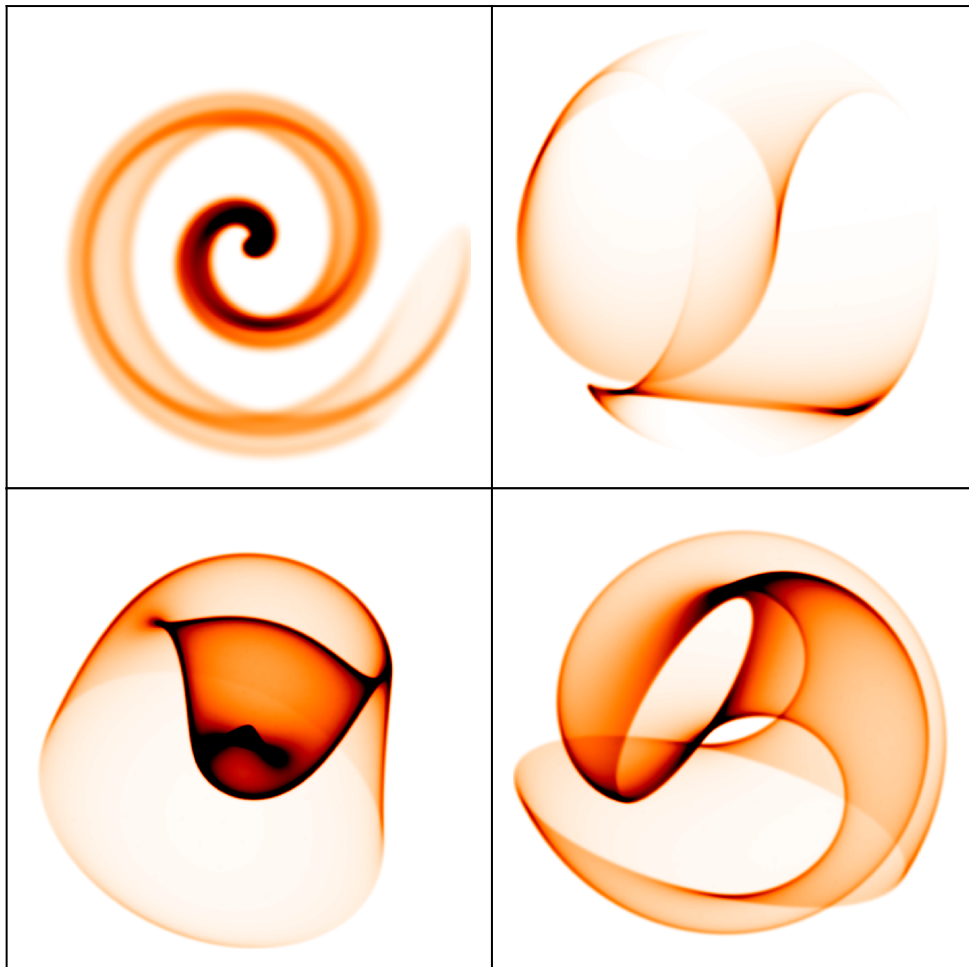


Fig. 8 Despite being the result of essentially the same physics, the colliding wind nebulae are able to take on strikingly different apparent forms. From left to right, top down, this mosaic shows simulated nebulae of WR 104, WR 140, WR 112, and Apep using the current best values for wind and orbital parameters in the literature.

although it is revealed as a site of strong dust formation through its infrared photometry and spectra. Despite having no image, the period and eccentricity of the orbit suggests that it may have similar structure to the nebulae of WR 140.

WR 48a At present, this is the only other candidate WR+WR CWB – specifically of WC8+WN8h classification (Zhekov et al., 2014) – and found in an orbit with eccentricity $e \sim 0.6$ (Williams et al., 2012). This was among the first objects to be identified as a colliding wind binary (Danks et al., 1983), and was first directly imaged in Marchenko and Moffat (2007). Like Apep, WR 48a has a relatively long orbital period of ~ 32 years and displays variable dust production throughout its orbit (although there is no evidence of a complete dust ‘turn off’ in 48a analogous to that in Apep).

Apep One of the only confirmed WR+WR systems, and certainly the only such to harbour a WC with a dust nebula (Callingham et al., 2020), Apep (WR 70-16) was identified as a bright X-ray and radio source and is potentially the brightest of all the CWBs. It has been observed with the VLT in the mid-infrared which revealed its spiral dust nebula structure (Callingham et al., 2019; Han et al., 2020). Also a likely triple system, an O8 star lies very close ($0.7''$) to the north of the WR+WR inner binary with evidence that indicates physical association.

WR 98a One of the first colliding wind nebulae to be directly imaged, this system showed the first imaging evidence of inclination effects in a pinwheel nebula (Monnier et al., 1999), in contrast to the Archimedean spiral of WR 104.

WR 104 As the first colliding wind binary to be directly imaged at high angular resolution, WR 104 emerged as the prototype ‘pinwheel nebula’ from the clear evidence of orbital motion in its dust plume (Tuthill et al., 1999). This system has been the subject of intense study, particularly in hydrodynamical simulations and the application of pinwheel structure to other CWB nebulae. Like WR 98a, WR 104 is a reasonably short period WC+O binary ($\lesssim 2$ years) in a very circular orbit (Tuthill et al., 2008). Recently, a B star distant from the WC+O binary was considered as being associated with the system (Wallace et al., 2002; Soulain et al., 2018), potentially making WR 104 one of the very few known WR triple systems. Hill (2024) suggested that the binary orbit may in fact be moderately inclined from our perspective (inclination $i > 34^\circ$: a finding that, at face value, is difficult to reconcile with the face-on fits $i < 16^\circ$ from imagery). Any resolution to this puzzle remains outstanding at the time of writing.

WR 112 First imaged in 2002, the colliding wind nebula of WR 112 was the first to visibly reveal concentric shells of dust formation (Marchenko et al., 2002) from its inner WC8+O binary (Lau et al., 2020). Like the other consistent dust producers listed here (WR 98a, 104), WR 112 has a well constrained eccentricity close to 0 as is evident from its regular concentric shell structure. Notably, the pinwheel nebula structure was incorrectly applied to WR 112’s dust nebula twice, yielding far-off estimates of the nebula expansion speed and the binary eccentricity and inclination (Marchenko et al., 2002; Lau et al., 2017).

WR 125 One of the longer period colliding wind binaries, the WC7+O9III binary shows episodic dust production with a periodicity of 28.1 years (Endo et al., 2022; Richardson et al., 2024). While not yet imaged, the surrounding dust shell has been suggested as anisotropic and the binary orbit elliptical (Richardson et al., 2024).

WR 137 One of the three original systems first catalogued by French astronomers Charles Wolf and Georges Rayet in 1867 (Wolf and Rayet, 1867), WR 137 is a WC7+O9V colliding wind binary (Richardson et al., 2016). The infrared light curve shows episodic dust production over an orbital period of about 13.1 years, and the orbital plane of the binary appears to be almost entirely in the line of sight (Peatt et al., 2023; Lau et al., 2024).

WR 140 The ‘prototype’ colliding wind binary, composed of WC8+O5 stars on a very high eccentricity ($e \sim 0.89$) orbit of about 7.9 years (Williams et al., 2009a; Monnier et al., 2011). This was the first system to be unequivocally identified as a colliding wind binary, largely due to its strongly modulated dust production: the dust seen in Figure 7 (right-side) is produced only in a narrow time frame as the stars approach and leave periastron (Lau et al., 2022; Han et al., 2022), and this reliably repeats on each orbital passage. This is perhaps the most well studied of all CWBs across all wavelengths and imaging techniques.

WR 147 An apparent triple system composed of a WN8, a close unseen companion, and a distant OB star (Rodríguez et al., 2020). This is the first system to have an observed pinwheel from the inner binary not in the infrared but in the radio. Furthermore there is a well resolved bow-shock distinct from the pinwheel where the winds collide with the ternary component. This aligns with previous X-ray observations that resolved the system as a double X-ray source: one at the inner binary and another at the WCR of the inner binary relative to the outer companion (Zhekov and Park, 2010b,a).

4 Implications and Fate

4.1 Wolf-Rayet Binaries as Supernova Progenitors

Wolf-Rayet stars are convincing candidates for Type Ib/Ic supernovae (SNe Ibc) progenitors: WRs are massive pre-supernova stars that lack hydrogen spectra, as do SNe Ibc (Filippenko, 1997; Crowther, 2007; McClelland and Eldridge, 2016). There is some discussion of an alternate SNe Ibc channel in Smartt (2009) where a lower mass star may lose its hydrogen envelope via binary interactions prior to undergoing supernova (not dissimilar to one of the proposed channels of WR formation; Paczyński, 1967). The consensus is that at least some combination of the WR progenitor model and this alternate scenario explain the observed population of SNe Ibc (see: Eldridge et al., 2013; Pellegrino et al., 2022; Karamahmetoglu et al., 2023).

Despite their intuitive connection, no WR stars have been definitively shown to be SNe Ibc progenitors with pre-supernova imaging of galaxies. Kilpatrick et al. (2021) identified the likely progenitor of Type Ib supernova SN2019yvr in *Hubble Space Telescope* imagery taken 2.6 yr prior to explosion. They found that neither a clear-cut WR nor a lower mass binary can adequately describe the SN progenitor, indicating that perhaps a sudden change in the observables of SNe Ibc progenitors take place just prior to explosion, e.g. extreme mass

loss. The lack of attribution could also plausibly be ascribed at least in part to the reduced detectability of WR stars at extragalactic distance (Pledger et al., 2021).

On the other hand, connections have been made between Type Ic supernovae and gamma-ray bursts (GRBs). Gamma-ray bursts are a class of energetic transient whose durations distinctly fall into two categories of ‘short’ and ‘long’, with several sources appearing isotropically on the sky each day (Woosley and Bloom, 2006). Short GRBs, of order $\lesssim 2$ s, are understood to be the result of kilonovae, the breakup of degenerate neutron stars during gravitational wave induced binary inspiral (Berger, 2014). In contrast, long GRBs (LGRBs), of order $\gtrsim 2$ s, arise from the relativistic jets produced in the core-collapse of highly rotating massive stars (Woosley and Heger, 2006). In fact, several SNe Ic-BL events, SNe Ic with especially broad spectral lines indicative of relativistic ejecta, have been definitively associated with LGRBs and fast X-ray bursts (Galama et al., 1998; Ashall et al., 2019; van Dalen et al., 2024). Interestingly, not all of these SNe Ic-BL have been associated with LGRBs, indicating that either the jets are highly collimated (and hence their visibility being very direction dependent) or there remains a significant gap in understanding (Siebert et al., 2024; van Dalen et al., 2024).

The consensus on the LGRB mechanism is in the collapsar model, where at the time of supernova the innermost core collapses into a black hole (BH). The surrounding core, having a high enough angular momentum to form a disc, produces polar jets as a result of angular momentum loss as matter accretes onto the natal BH (Woosley, 1993; Dean and Fernández, 2024). For a star to do this, it must be rotating extremely rapidly. This should be the case for stars that have been efficiently mixed during their lifetimes (Woosley and Heger, 2006), and hence stars that are effectively free of hydrogen at supernova as a result. Therefore it is not a requirement that GRBs have no hydrogen line association (and hence a Type I vs a Type II SN), but rather a consequence of the evolutionary process that gives rise to GRBs. Because of this, helium and metal-rich stars emerge as the leading candidate progenitors for SNe Ic-BL. There is a significant body of simulations linking WR to SNe Ic and GRBs through the collapsar model (McClelland and Eldridge, 2016; Aguilera-Dena et al., 2018), especially those with high rotation at preferentially low metallicity (Detmers et al., 2008).

4.1.1 Metallicity in Different Epochs

Modern Wolf-Rayet stars are synonymous with metallic line-driven winds. These winds, along with magnetic effects, are known to be efficient at dissipating angular momentum from hot stars (Woosley and Heger, 2006; Ud-Doula et al., 2009). This, in conjunction with the more efficient mass-loss at high metallicity (Vink and de Koter, 2005; Gräfener and Hamann, 2008), means that we generally expect Galactic WRs to be slower rotators than those in less-evolved galaxies. There is a strong dependence on the rotation speed of a progenitor star to its LGRB status (and also between the spin of the collapsar BH to the GRB jet collimation; Hurtado et al., 2024), and so the logical conclusion is that we should expect fewer or no LGRBs in evolved galaxies with high metal content.

Indeed, there is strong indication from stellar models that low-metallicity massive stars should be rapidly rotating (Chiappini et al., 2006; Vink and Harries, 2017). This motivates searches for LGRB progenitors in dwarf and/or satellite galaxies where the metal content can be orders of magnitude below solar metallicity (Tolstoy et al., 2009). There has been some plausible, if inconclusive, evidence of rapidly-rotating WRs in the Large Magellanic Cloud (Shenar et al., 2014; Vink and Harries, 2017), lending credence to this idea. Therefore we expect that LGRBs are efficiently produced in the early universe or in dwarf galaxies with less enriched chemical content.

One proposed channel for fast spinning massive stars, and hence LGRB events, within chemically evolved galaxies like the Milky Way is in the tidal spin up from a closely orbiting companion star. Early studies suggest that this mechanism is improbable at solar metallicity and marginally more likely at low metallicity (Detmers et al., 2008). More recently, population synthesis studies have shown this to be an efficient mechanism to sustain fast rotation in evolved stars (Chrimes et al., 2020; Bavera et al., 2022), although only in very closely orbiting binaries. While most observed evolved Wolf-Rayet stars are not in close binaries, a select few (namely WR 140 and Apep) are in highly eccentric orbits which brings the two component stars together at periastron. It is unclear how these close passages affect the rotation and internal structure of the WR stars, and if this allows for a tidal spin-up.

4.1.2 Supernovae in Binaries and Effects of Circumstellar Material

Regardless of the stellar rotation properties, a significant fraction of Wolf-Rayet stars exist in binaries and their supernova explosions are astrophysically imminent. If a Wolf-Rayet supernova occurs in a colliding wind binary system, especially one with a prominent infrared excess, there will be a rich circumstellar structure surrounding the system from previous epochs of dust production. After supernova begins and light begins emanating from its source, the surrounding material may become luminous (with some delay from the explosion) by the ‘light echo’ phenomenon (van den Bergh, 1965; Crotts et al., 1995).

The radial extent of the colliding wind nebulae discussed earlier are determined mainly by two parameters: the expansion velocity and the orbital period. In this way, any light echo inherent to this circumstellar nebula structure would have an emission delay proportional to each of these parameters and the speed of light. A consequence of this periodic shell circumstellar medium (CSM) structure is that the supernova light curve should also display some periodicity in its light echo (or in the repeated SN ejecta-CSM contact). Moore et al. (2023) report the first unambiguous detection of such a light curve in the optical, with a ~ 12.5 day modulation of brightness. This supernova, SN 2022jli, was also of the Type Ic subtype indicative of a Wolf-Rayet progenitor; further, the required CSM mass is consistent with typical WR mass loss rates. Similar quasi-periodic bumps in brightness have been observed in SN 2015bn (Nicholl et al., 2016), SN 2020qlb (West et al., 2023), and SN 2023aew (Kangas et al., 2024), among others, which are all hydrogen-poor SNe albeit with higher time intervals between light curve bumps than in SN 2022jli.

Turning away from the optical emission from supernovae and into the radio, unambiguous periodic oscillations in brightness have been observed twice before: in SN 1979C (Weiler et al., 1991, 1992) and in SN 2001ig (Ryder et al., 2004). As of yet, there has been no definite periodic radio emission observed around a SNe Ibc, although SN 2007bg likely shows evidence of a structured CSM through its

radio emission (Salas et al., 2013). No matter the supernova subtype, there is evidence across the electromagnetic spectrum indicating a structured circumstellar medium surrounding massive, evolved stars. While ejecta interactions with stellar mass eruptions may support a subset of these observations, the nested rungs of regular dust shells created from colliding wind binaries provide the most natural explanation for these environments.

5 Summary and Outlook

Colliding wind binaries, especially those hosting a Wolf-Rayet star, open a new window into otherwise inaccessible stellar physics. The wind-wind shock between the stars allows us to better understand the properties of each stellar wind, and in turn offers a rich landscape of observable phenomenology that yields diagnostics and probes into the final phases of massive stars immediately before undergoing supernova explosions. These wind collision shocks are bright non-thermal emitters in the X-ray and at radio frequencies, and can be luminous in the infrared and sub-millimetre in cases where the production of copious warm dust is nucleated from gas in the streaming wind. With many examples offering a panoply of intricately structured observational signatures, the Wolf-Rayet CWBs offer a fascinating astrophysical laboratory open to studies across the electromagnetic spectrum.

Every year, more Wolf-Rayet colliding wind binaries are discovered in the Galaxy, the Magellanic Clouds and increasingly at intergalactic distances. As higher cadence and wider field photometric surveys come online, our understanding of the spatial distribution of CWBs as well as their time-evolving behaviour will come under close observational scrutiny. In parallel, sensitive infrared and sub-millimetre observatories such as JWST and ALMA offer a new avenue to progress our understanding of the orbits of these stars and the geometries of their nebulae. Although the separation of the binary stars themselves is usually too close and/or the system too obscured to be directly resolved, the fast wind delivers a remarkable gift to observers. Complex structures encoding detailed colliding-wind physics, engraved at sub-milliarcsecond scales, are preserved and inflated within the spherically expanding nebula, leaving a fossil record witnessing hundreds of years of system evolution written across the sky at arcsecond scales. While contemporary work has delivered remarkable success in fitting these data with simple geometrical models, a synthesis with physically motivated elements from hydrodynamics and radiative transfer will be required to understand upcoming and archival direct imagery.

Given the disproportionate importance played in the cosmic ecosystem by the most massive of stars – which drive radiation, winds and supernova ejecta at galactic scales – astronomy is fortunate to have the colliding wind binaries. Each forms a distinct and richly featured laboratory boasting diagnostics accessible across the electromagnetic spectrum for confronting model scenarios, constraining basic properties and yielding insight into this fleeting yet critical phase in the lives of massive stars.

Acknowledgements

We thank Benjamin Pope, Yinuo Han and Peredur Williams for helpful discussions, suggestions, and feedback throughout the writing of this work. RMTW acknowledges the financial support of the Andy Thomas Space Foundation.

References

- Abbott DC and Conti PS (1987), Jan. Wolf-rayet stars. *ARA&A* 25: 113–150. doi:10.1146/annurev.aa.25.090187.000553.
- Aguilera-Dena DR, Langer N, Moriya TJ and Schootemeijer A (2018), May. Related Progenitor Models for Long-duration Gamma-Ray Bursts and Type Ic Superluminous Supernovae. *ApJ* 858 (2), 115. doi:10.3847/1538-4357/aabfc1. 1804.07317.
- Allen DA, Swings JP and Harvey PM (1972), Jan. Infrared photometry of northern Wolf-Rayet stars. *A&A* 20: 333.
- Archimedes (2017), Contents, Netz R, (Ed.), *The Works of Archimedes: Translation and Commentary*, Cambridge University Press.
- Ashall C, Mazzali PA, Pian E, Woosley SE, Palazzi E, Prentice SJ, Kobayashi S, Holmbo S, Levan A, Perley D, Stritzinger MD, Bufano F, Filippenko AV, Melandri A, Oates S, Rossi A, Selsing J, Zheng W, Castro-Tirado AJ, Chincarini G, D’Avanzo P, De Pasquale M, Emery S, Fruchter AS, Hurley K, Moller P, Nomoto K, Tanaka M and Valeev AF (2019), Aug. GRB 161219B/SN 2016jca: a powerful stellar collapse. *MNRAS* 487 (4): 5824–5839. doi:10.1093/mnras/stz1588. 1702.04339.
- Barlow MJ, Smith LJ and Willis AJ (1981), Jul. Mass-loss rates for 21 Wolf-rayet stars. *MNRAS* 196: 101–110. doi:10.1093/mnras/196.2.101.
- Baug T, de Grijs R, Dewangan LK, Herczeg GJ, Ojha DK, Wang K, Deng L and Bhatt BC (2019), Nov. Influence of Wolf-Rayet Stars on Surrounding Star-forming Molecular Clouds. *ApJ* 885 (1), 68. doi:10.3847/1538-4357/ab46be. 1909.01996.
- Bavera SS, Fragos T, Zapartas E, Ramirez-Ruiz E, Marchant P, Kelley LZ, Zevin M, Andrews JJ, Coughlin S, Dotter A, Kovlakas K, Misra D, Serra-Perez JG, Qin Y, Rocha KA, Román-Garza J, Tran NH and Xing Z (2022), Jan. Probing the progenitors of spinning binary black-hole mergers with long gamma-ray bursts. *A&A* 657, L8. doi:10.1051/0004-6361/202141979. 2106.15841.
- Benaglia P, De Becker M, Ishwara-Chandra CH, Intema HT and Isequilla NL (2020), Jul. Megahertz emission of massive early-type stars in the Cygnus region. *PASA* 37, e030. doi:10.1017/pasa.2020.21. 2006.00867.
- Berger E (2014), Aug. Short-Duration Gamma-Ray Bursts. *ARA&A* 52: 43–105. doi:10.1146/annurev-astro-081913-035926. 1311.2603.
- Blanco AB, De Becker M, Saha A, Tej A and Benaglia P (2024), Oct. Insight into the occurrence of particle acceleration through the investigation of Wolf-Rayet stars using uGMRT observations. *A&A* 690, A78. doi:10.1051/0004-6361/202451161. 2408.07640.
- Bonanos AZ, Stanek KZ, Udalski A, Wyrzykowski L, Żebruń K, Kubiak M, Szymański MK, Szewczyk O, Pietrzyński G and Soszyński I (2004), Aug. WR 20a Is an Eclipsing Binary: Accurate Determination of Parameters for an Extremely Massive Wolf-Rayet System. *ApJ* 611 (1): L33–L36. doi:10.1086/423671. astro-ph/0405338.
- Callingham JR, Gaensler BM, Ekers RD, Tingay SJ, Wayth RB, Morgan J, Bernardi G, Bell ME, Bhat R, Bowman JD, Briggs F, Cappallo RJ, Deshpande AA, Ewall-Wice A, Feng L, Greenhill LJ, Hazelton BJ, Hindson L, Hurley-Walker N, Jacobs DC, Johnston-Hollitt M, Kaplan

- DL, Kudrayvtseva N, Lenc E, Lonsdale CJ, McKinley B, McWhirter SR, Mitchell DA, Morales MF, Morgan E, Oberoi D, Offringa AR, Ord SM, Pindor B, Prabu T, Procopio P, Riding J, Srivani KS, Subrahmanyan R, Udaya Shankar N, Webster RL, Williams A and Williams CL (2015), Aug. Broadband Spectral Modeling of the Extreme Gigahertz-peaked Spectrum Radio Source PKS B0008-421. *ApJ* 809 (2), 168. doi:10.1088/0004-637X/809/2/168. 1507.04819.
- Callingham JR, Tuthill PG, Pope BJS, Williams PM, Crowther PA, Edwards M, Norris B and Kedziora-Chudczer L (2019), Mar. Anisotropic winds in a Wolf-Rayet binary identify a potential gamma-ray burst progenitor. *Nature Astronomy* 3: 82–87. doi:10.1038/s41550-018-0617-7. 1811.06985.
- Callingham JR, Crowther PA, Williams PM, Tuthill PG, Han Y, Pope BJS and Marcote B (2020), Jan. Two Wolf-Rayet stars at the heart of colliding-wind binary Apep. *MNRAS* 495 (3): 3323–3331. doi:10.1093/mnras/staa1244. 2005.00531.
- Cameron AJ, Katz H, Witten C, Saxena A, Laporte N and Bunker AJ (2024), Oct. Nebular dominated galaxies: insights into the stellar initial mass function at high redshift. *MNRAS* 534 (1): 523–543. doi:10.1093/mnras/stae1547. 2311.02051.
- Carroll BW and Ostlie DA (2017). *An Introduction to Modern Astrophysics*, Second Edition, Cambridge University Press.
- Castor JI, Abbott DC and Klein RI (1975), Jan. Radiation-driven winds in Of stars. *ApJ* 195: 157–174. doi:10.1086/153315.
- Chené AN, St-Louis N, Moffat AFJ and Gayley KG (2020), Nov. Clumping in the Winds of Wolf-Rayet Stars. *ApJ* 903 (2), 113. doi:10.3847/1538-4357/abba24. 2009.10341.
- Cherchneff I, Le Teuff YH, Williams PM and Tielens AGGM (2000), May. Dust formation in carbon-rich Wolf-Rayet stars. I. Chemistry of small carbon clusters and silicon species. *A&A* 357: 572–580.
- Cherepashchuk AM (1976), Aug. Detectability of Wolf-Rayet binaries from X-rays. *Soviet Astronomy Letters* 2: 138.
- Chiappini C, Hirschi R, Meynet G, Ekström S, Maeder A and Matteucci F (2006), Apr. A strong case for fast stellar rotation at very low metallicities. *A&A* 449 (2): L27–L30. doi:10.1051/0004-6361/20064866. astro-ph/0602459.
- Chrimas AA, Stanway ER and Eldridge JJ (2020), Jan. Binary population synthesis models for core-collapse gamma-ray burst progenitors. *MNRAS* 491 (3): 3479–3495. doi:10.1093/mnras/stz3246. 1911.08387.
- Cichowolski S, Suad LA, Pineault S, Noriega-Crespo A, Arnal EM and Flagey N (2015), Jul. The infrared and molecular environment surrounding the Wolf-Rayet star WR 130. *MNRAS* 450 (4): 3458–3471. doi:10.1093/mnras/stv826. 1504.04526.
- Condon JJ (1992), Jan. Radio emission from normal galaxies. *ARA&A* 30: 575–611. doi:10.1146/annurev.aa.30.090192.003043.
- Conti PS (1975), Jan. On the relationship between Of and WR stars. *Memoires of the Societe Royale des Sciences de Liege* 9: 193–212.
- Crotts APS, Kunkel WE and Heathcote SR (1995), Jan. The Circumstellar Envelope of SN 1987A. I. The Shape of the Double-lobed Nebula and Its Rings and the Distance to the Large Magellanic Cloud. *ApJ* 438: 724. doi:10.1086/175117.
- Crowther PA (2007), Sep. Physical Properties of Wolf-Rayet Stars. *ARA&A* 45 (1): 177–219. doi:10.1146/annurev.astro.45.051806.110615. astro-ph/0610356.
- Dale JE, Ngoumou J, Ercolano B and Bonnell IA (2013), Dec. Massive stars in massive clusters - IV. Disruption of clouds by momentum-driven winds. *MNRAS* 436 (4): 3430–3445. doi:10.1093/mnras/stt1822. 1309.7355.
- Danks AC, Dennefeld M, Wamsteker W and Shaver PA (1983), Feb. Near infrared spectroscopy and infrared photometry of a new WC9 star. *A&A* 118: 301–305.
- De Becker M (2007), Nov. Non-thermal emission processes in massive binaries. *A&A Rev.* 14 (3-4): 171–216. doi:10.1007/s00159-007-0005-2. 0709.4220.
- De Becker M and Rauco F (2013), Oct. Catalogue of particle-accelerating colliding-wind binaries. *A&A* 558, A28. doi:10.1051/0004-6361/201322074. 1308.3149.
- De Marco O and Izzard RG (2017), Jan. Dawes Review 6: The Impact of Companions on Stellar Evolution. *PASA* 34, e001. doi:10.1017/pasa.2016.52. 1611.03542.
- De Marco O and Schmutz W (1999), May. The γ Velorum binary system. I. O star parameters and light ratio. *A&A* 345: 163–171.
- De Marco O, Schmutz W, Crowther PA, Hillier DJ, Dessart L, de Koter A and Schweickhardt J (2000), Jun. The γ Velorum binary system. II. WR stellar parameters and the photon loss mechanism. *A&A* 358: 187–200. doi:10.48550/arXiv.astro-ph/0004081. astro-ph/0004081.
- Dean C and Fernández R (2024), Apr. Collapsar disk outflows: Viscous hydrodynamic evolution in axisymmetry. *Phys. Rev. D* 109 (8), 083010. doi:10.1103/PhysRevD.109.083010. 2403.08877.
- de Koter A, Heap SR and Hubeny I (1997), Mar. On the Evolutionary Phase and Mass Loss of the Wolf-Rayet-like Stars in R136a. *ApJ* 477: 792. doi:10.1086/303736.
- Detmers RG, Langer N, Podsiadlowski P and Izzard RG (2008), Jun. Gamma-ray bursts from tidally spun-up Wolf-Rayet stars? *A&A* 484 (3): 831–839. doi:10.1051/0004-6361/200809371. 0804.0014.
- de Wit WJ, Testi L, Palla F and Zinnecker H (2005), Jul. The origin of massive O-type field stars: II. Field O stars as runaways. *A&A* 437 (1): 247–255. doi:10.1051/0004-6361/20042489. astro-ph/0503337.
- Dougherty SM, Beasley AJ, Claussen MJ, Zauderer BA and Bolingbroke NJ (2005), Apr. High-Resolution Radio Observations of the Colliding-Wind Binary WR 140. *ApJ* 623 (1): 447–459. doi:10.1086/428494. astro-ph/0501391.
- Dsilva K, Shenar T, Sana H and Marchant P (2020), Sep. A spectroscopic multiplicity survey of Galactic Wolf-Rayet stars. I. The northern WC sequence. *A&A* 641, A26. doi:10.1051/0004-6361/202038446. 2006.13957.
- Dsilva K, Shenar T, Sana H and Marchant P (2022), Aug. A spectroscopic multiplicity survey of Galactic Wolf-Rayet stars. II. The northern WNE sequence. *A&A* 664, A93. doi:10.1051/0004-6361/202142729. 2204.12518.
- Dsilva K, Shenar T, Sana H and Marchant P (2023), Jun. A spectroscopic multiplicity survey of Galactic Wolf-Rayet stars. III. The northern late-type nitrogen-rich sample. *A&A* 674, A88. doi:10.1051/0004-6361/202244308. 2212.06927.
- Eatson JW, Pittard JM and Van Loo S (2022a), Nov. An exploration of dust grain growth within WCd systems using an advected scalar dust model. *MNRAS* 516 (4): 6132–6144. doi:10.1093/mnras/stac2617. 2204.07397.
- Eatson JW, Pittard JM and Van Loo S (2022b), Dec. Exploring dust growth in the episodic WCd system WR140. *MNRAS* 517 (4): 4705–4713. doi:10.1093/mnras/stac3000. 2204.12354.
- Eichler D and Usov V (1993), Jan. Particle Acceleration and Nonthermal Radio Emission in Binaries of Early-Type Stars. *ApJ* 402: 271. doi:10.1086/172130.
- Eldridge JJ, Langer N and Tout CA (2011), Jul. Runaway stars as progenitors of supernovae and gamma-ray bursts. *MNRAS* 414 (4): 3501–3520. doi:10.1111/j.1365-2966.2011.18650.x. 1103.1877.
- Eldridge JJ, Fraser M, Smartt SJ, Maund JR and Crockett RM (2013), Nov. The death of massive stars - II. Observational constraints on the progenitors of Type Ibc supernovae. *MNRAS* 436 (1): 774–795. doi:10.1093/mnras/stt1612. 1301.1975.
- Endo I, Lau RM, Sakon I, Onaka T, Williams PM and Shenavrin VI (2022), May. Detection of a Broad 8 μ m UIR Feature in the Mid-infrared Spectrum of WR 125 Observed with Subaru/COMICS. *ApJ* 930 (2), 116. doi:10.3847/1538-4357/ac63bd. 2204.13259.
- Filippenko AV (1997), Jan. Optical Spectra of Supernovae. *ARA&A* 35: 309–355. doi:10.1146/annurev.astro.35.1.309.
- Foellmi C, Moffat AFJ and Guerrero MA (2003), Feb. Wolf-Rayet binaries in the Magellanic Clouds and implications for massive-star evolution -

- II. Large Magellanic Cloud. *MNRAS* 338 (4): 1025–1056. doi:10.1046/j.1365-8711.2003.06161.x.
- Galama TJ, Vreeswijk PM, van Paradijs J, Kouveliotou C, Augusteijn T, Bönhardt H, Brewer JP, Doublier V, Gonzalez JF, Leibundgut B, Lidman C, Hainaut OR, Patat F, Heise J, in't Zand J, Hurley K, Groot PJ, Strom RG, Mazzali PA, Iwamoto K, Nomoto K, Umeda H, Nakamura T, Young TR, Suzuki T, Shigeyama T, Koshut T, Kippen M, Robinson C, de Wildt P, Wijers RAMJ, Tanvir N, Greiner J, Pian E, Palazzi E, Frontera F, Masetti N, Nicastro L, Feroci M, Costa E, Piro L, Peterson BA, Tinney C, Boyle B, Cannon R, Stathakis R, Sadler E, Begam MC and Ianna P (1998), Oct. An unusual supernova in the error box of the γ -ray burst of 25 April 1998. *Nature* 395 (6703): 670–672. doi:10.1038/27150.astro-ph/9806175.
- Gamow G (1943), Nov. On WC and WN Stars. *ApJ* 98: 500. doi:10.1086/144581.
- Gayley KG (2009), Sep. Asymptotic Opening Angles for Colliding-Wind Bow Shocks: The Characteristic-Angle Approximation. *ApJ* 703 (1): 89–95. doi:10.1088/0004-637X/703/1/89.0905.1395.
- Gehrz RD and Hackwell JA (1974), Dec. Circumstellar dust emission from WC9 stars. *ApJ* 194: 619–622. doi:10.1086/153281.
- Gosset E and Nazé Y (2016), May. The X-ray light curve of the massive colliding wind Wolf-Rayet + O binary WR 21a. *A&A* 590, A113. doi:10.1051/0004-6361/201527051.1604.01536.
- Gräfener G and Hamann WR (2008), May. Mass loss from late-type WN stars and its Z-dependence. Very massive stars approaching the Eddington limit. *A&A* 482 (3): 945–960. doi:10.1051/0004-6361/20066176.0803.0866.
- Gräfener G, Vink JS, de Koter A and Langer N (2011), Nov. The Eddington factor as the key to understand the winds of the most massive stars. Evidence for a Γ -dependence of Wolf-Rayet type mass loss. *A&A* 535, A56. doi:10.1051/0004-6361/201116701.1106.5361.
- Grimaldo E, Reimer A, Kissmann R, Niederwanger F and Reitberger K (2019), Jan. Proton Acceleration in Colliding Stellar Wind Binaries. *ApJ* 871 (1), 55. doi:10.3847/1538-4357/aaf6ee.1812.02960.
- Groh JH, Meynet G, Georgy C and Ekström S (2013), Oct. Fundamental properties of core-collapse supernova and GRB progenitors: predicting the look of massive stars before death. *A&A* 558, A131. doi:10.1051/0004-6361/201321906.1308.4681.
- Hackwell JA, Gehrz RD, Smith JR and Strecker DW (1976), Nov. Infrared light variations of Wolf-Rayet stars. *ApJ* 210: 137–142. doi:10.1086/154811.
- Hamann WR, Gräfener G and Liermann A (2006), Oct. The Galactic WN stars. Spectral analyses with line-blanketed model atmospheres versus stellar evolution models with and without rotation. *A&A* 457 (3): 1015–1031. doi:10.1051/0004-6361/20065052.astro-ph/0608078.
- Han Y, Tuthill PG, Lau RM, Soulain A, Callingham JR, Williams PM, Crowther PA, Pope BJS and Marcote B (2020), Nov. The extreme colliding-wind system Apep: resolved imagery of the central binary and dust plume in the infrared. *MNRAS* 498 (4): 5604–5619. doi:10.1093/mnras/staa2349.2008.05834.
- Han Y, Tuthill PG, Lau RM and Soulain A (2022), Oct. Radiation-driven acceleration in the expanding WR140 dust shell. *Nature* 610 (7931): 269–272. doi:10.1038/s41586-022-05155-5.2210.06556.
- Harries TJ, Babler BL and Fox GK (2000), Sep. The polarized spectrum of the dust producing Wolf-Rayet+O-star binary WR137. *A&A* 361: 273–282.
- Harries TJ, Monnier JD, Symington NH and Kurosawa R (2004), May. Three-dimensional dust radiative-transfer models: the Pinwheel Nebula of WR 104. *MNRAS* 350 (2): 565–574. doi:10.1111/j.1365-2966.2004.07668.x.astro-ph/0401574.
- Hendrix T, Keppens R, van Marle AJ, Camps P, Baes M and Meliani Z (2016), Aug. Pinwheels in the sky, with dust: 3D modelling of the Wolf-Rayet 98a environment. *MNRAS* 460 (4): 3975–3991. doi:10.1093/mnras/stw1289.1605.09239.
- Hill GM (2024), Nov. Is WR 104 a face-on, colliding-wind binary? *MNRAS* 534 (3): 2184–2195. doi:10.1093/mnras/stae2183.
- Huber D, Kissmann R, Reimer A and Reimer O (2021), Feb. Relativistic fluid modelling of gamma-ray binaries. I. The model. *A&A* 646, A91. doi:10.1051/0004-6361/202039277.2012.04975.
- Hurtado VU, Lloyd-Ronning NM and Miller JM (2024), May. The Dependence of Gamma-Ray Burst Jet Collimation on Black Hole Spin. *ApJ* 967 (1), L4. doi:10.3847/2041-8213/ad3dfd.2309.07999.
- Josiek J, Ekström S and Sander AAC (2024), Apr. Impact of main-sequence mass loss on the appearance, structure and evolution of Wolf-Rayet stars. *arXiv e-prints*, arXiv:2404.14488doi:10.48550/arXiv.2404.14488.2404.14488.
- Kangas T, Kuncarayakti H, Nagao T, Kotak R, Kankare E, Fraser M, Stevance H, Mattila S, Maeda K, Stritzinger M, Lundqvist P, Elias-Rosa N, Ferrari L, Folatelli G, Frohmaier C, Galbany L, Kawabata M, Koutsionia E, Müller-Bravo TE, Pursiainen M, Singh A, Taguchi K, Teja RS, Valerin G, Pastorello A, Benetti S, Cai YZ, Charalampopoulos P, Gutiérrez CP, Kravtsov T and Reguitti A (2024), Sep. The enigmatic double-peaked stripped-envelope SN 2023aew. *A&A* 689, A182. doi:10.1051/0004-6361/202449420.2401.17423.
- Karamehmetoglu E, Sollerman J, Taddia F, Barbarino C, Feindt U, Fremling C, Gal-Yam A, Kasliwal MM, Petrushevska T, Schulze S, Stritzinger MD and Zapartas E (2023), Oct. A population of Type Ibc supernovae with massive progenitors. Broad lightcurves not uncommon in (i)PTF. *A&A* 678, A87. doi:10.1051/0004-6361/202245231.2210.09402.
- Kellermann KI (1966), Apr. The radio source 1934-63. *Australian Journal of Physics* 19: 195. doi:10.1071/PH660195.
- Kilpatrick CD, Drout MR, Auchettl K, Dimitriadis G, Foley RJ, Jones DO, DeMarchi L, French KD, Gall C, Hjorth J, Jacobson-Galán WV, Margutti R, Piro AL, Ramirez-Ruiz E, Rest A and Rojas-Bravo C (2021), Jun. A cool and inflated progenitor candidate for the Type Ib supernova 2019yvr at 2.6 yr before explosion. *MNRAS* 504 (2): 2073–2093. doi:10.1093/mnras/stab838.2101.03206.
- Kroupa P (2001), Apr. On the variation of the initial mass function. *MNRAS* 322 (2): 231–246. doi:10.1046/j.1365-8711.2001.04022.x.astro-ph/0009005.
- Lamberts A, Dubus G, Lesur G and Fromang S (2012), Oct. Impact of orbital motion on the structure and stability of adiabatic shocks in colliding wind binaries. *A&A* 546, A60. doi:10.1051/0004-6361/201219006.1202.2060.
- Lamberts A, Millour F, Liermann A, Dessart L, Driebe T, Duvert G, Finsterle W, Girault V, Massi F, Petrov RG, Schmutz W, Weigelt G and Chesneau O (2017), Jul. Numerical simulations and infrared spectro-interferometry reveal the wind collision region in γ^2 Velorum. *MNRAS* 468 (3): 2655–2671. doi:10.1093/mnras/stx588.1701.01124.
- Lau RM, Hankins MJ, Schödel R, Sanchez-Bermudez J, Moffat AFJ and Ressler ME (2017), Feb. Stagnant Shells in the Vicinity of the Dusty Wolf-Rayet-OB Binary WR 112. *ApJ* 835 (2), L31. doi:10.3847/2041-8213/835/2/L31.1612.05650.
- Lau RM, Hankins MJ, Han Y, Endo I, Moffat AFJ, Ressler ME, Sakon I, Sanchez-Bermudez J, Soulain A, Stevens IR, Tuthill PG and Williams PM (2020), Sep. Resolving Decades of Periodic Spirals from the Wolf-Rayet Dust Factory WR 112. *ApJ* 900 (2), 190. doi:10.3847/1538-4357/abaab8.2008.01093.
- Lau RM, Hankins MJ, Kasliwal MM, Bond HE, De K, Jencson JE, Moffat AFJ, Smith N and Williams PM (2021), Mar. Revealing Efficient Dust Formation at Low Metallicity in Extragalactic Carbon-rich Wolf-Rayet Binaries. *ApJ* 909 (2), 113. doi:10.3847/1538-4357/abd8cd.2011.09732.
- Lau RM, Hankins MJ, Han Y, Argyriou I, Corcoran MF, Eldridge JJ, Endo I, Fox OD, Garcia Marin M, Gull TR, Jones OC, Hamaguchi K, Lamberts A, Law DR, Madura T, Marchenko SV, Matsuhara H, Moffat AFJ, Morris MR, Morris PW, Onaka T, Ressler ME, Richardson ND, Russell CMP, Sanchez-Bermudez J, Smith N, Soulain A, Stevens IR, Tuthill P, Weigelt G, Williams PM and Yamaguchi R (2022), Nov. Nested dust shells around the Wolf-Rayet binary WR 140 observed with JWST. *Nature Astronomy* 6: 1308–1316. doi:10.1038/s41550-022-01812-x.2210.06452.
- Lau RM, Wang J, Hankins MJ, Currie T, Deo V, Endo I, Guyon O, Han Y, Jones AP, Jovanovic N, Lozi J, Moffat AFJ, Onaka T, Ruane G, Sander

- AAC, Tinyanont S, Tuthill PG, Weigelt G, Williams PM and Vievard S (2023), Jul. From Dust to Nanodust: Resolving Circumstellar Dust from the Colliding-wind Binary Wolf-Rayet 140. *ApJ* 951 (2), 89. doi:10.3847/1538-4357/acd4c5. 2305.14557.
- Lau RM, Hankins MJ, Sanchez-Bermudez J, Thatte D, Soulain A, Cooper RA, Sivaramakrishnan A, Corcoran MF, Greenbaum AZ, Gull TR, Han Y, Jones OC, Madura T, Moffat AFJ, Morris MR, Onaka T, Russell CMP, Richardson ND, Smith N, Tuthill P, Volk K, Weigelt G and Williams PM (2024), Mar. A First Look with JWST Aperture Masking Interferometry: Resolving Circumstellar Dust around the Wolf-Rayet Binary WR 137 beyond the Rayleigh Limit. *ApJ* 963 (2), 127. doi:10.3847/1538-4357/ad192c. 2311.15948.
- Lefèvre L, Marchenko SV, Lépine S, Moffat AFJ, Acker A, Harries TJ, Annuik K, Bohlender DA, Demers H, Grosdidier Y, Hill GM, Morrison ND, Knauth DC, Skalkowski G and Viti S (2005), Jun. Spectroscopic study of the long-period dust-producing WC7pd+O9 binary HD 192641. *MNRAS* 360 (1): 141–152. doi:10.1111/j.1365-2966.2005.09057.x. astro-ph/0504475.
- Mackey J, Jones TAK, Brose R, Grassitelli L, Reville B and Mathew A (2023), Dec. Inverse-Compton cooling of thermal plasma in colliding-wind binaries. *MNRAS* 526 (2): 3099–3114. doi:10.1093/mnras/stad2839. 2301.13716.
- Marchenko SV and Moffat AFJ (2007), Jan., Dust Formation in Massive WR+O Binaries: Recent Results, St. -Louis N and Moffat AFJ, (Eds.), *Massive Stars in Interactive Binaries*, Astronomical Society of the Pacific Conference Series, 367, pp. 213, astro-ph/0610531.
- Marchenko SV, Moffat AFJ, Vacca WD, Côté S and Doyon R (2002), Jan. Massive Binary WR 112 and Properties of Wolf-Rayet Dust. *ApJ* 565 (1): L59–L62. doi:10.1086/339138. astro-ph/0112403.
- Marchenko SV, Moffat AFJ and Crowther PA (2010), Nov. Population I Wolf-Rayet Runaway Stars: The Case of WR124 and its Expanding Nebula M1-67. *ApJ* 724 (1): L90–L94. doi:10.1088/2041-8205/724/1/L90. 1011.0785.
- Marcote B, Callingham JR, De Becker M, Edwards PG, Han Y, Schulz R, Stevens J and Tuthill PG (2021), Feb. AU-scale radio imaging of the wind collision region in the brightest and most luminous non-thermal colliding wind binary Apep. *MNRAS* 501 (2): 2478–2486. doi:10.1093/mnras/staa3863. 2012.06571.
- McClelland LAS and Eldridge JJ (2016), Jun. Helium stars: towards an understanding of Wolf-Rayet evolution. *MNRAS* 459 (2): 1505–1518. doi:10.1093/mnras/stw618. 1602.06358.
- Meynet G, Georgy C, Hirschi R, Maeder A, Massey P, Przybilla N and Nieva MF (2011), Jan. Red Supergiants, Luminous Blue Variables and Wolf-Rayet stars: the single massive star perspective. *Bulletin de la Societe Royale des Sciences de Liege* 80: 266–278. doi:10.48550/arXiv.1101.5873. 1101.5873.
- Michaux YJL, Moffat AFJ, Chené AN and St-Louis N (2014), May. On the origin of variable structures in the winds of hot luminous stars. *MNRAS* 440 (1): 2–9. doi:10.1093/mnras/stt2102. 1312.2864.
- Miller GE and Scalo JM (1979), Nov. The Initial Mass Function and Stellar Birthrate in the Solar Neighborhood. *ApJS* 41: 513. doi:10.1086/190629.
- Millour F, Petrov RG, Chesneau O, Bonneau D, Dessart L, Bechet C, Tallon-Bosc I, Tallon M, Thiébaud E, Vakili F, Malbet F, Mourard D, Antonelli P, Beckmann U, Bresson Y, Chelli A, Dugué M, Duvert G, Gennari S, Glüch L, Kern P, Lagarde S, Le Coarer E, Lisi F, Perraut K, Puget P, Rantakyro F, Robbe-Dubois S, Roussel A, Tatulli E, Weigelt G, Zins G, Accardo M, Acke B, Agabi K, Altariba E, Arezki B, Aristidi E, Baffa C, Behrend J, Blöcker T, Bonhomme S, Busoni S, Cassaing F, Clause JM, Colin J, Connot C, Delboulbé A, Domiciano de Souza A, Driebe T, Feautrier P, Ferruzzi D, Forveille T, Fossat E, Foy R, Fraix-Burnet D, Gallardo A, Giani E, Gil C, Glentzlin A, Heiden M, Heining M, Hernandez Utrera O, Hofmann KH, Kamm D, Kiekebusch M, Kraus S, Le Contel D, Le Contel JM, Lesourd T, Lopez B, Lopez M, Magnard Y, Marconi A, Mars G, Martinot-Lagarde G, Mathias P, Mège P, Monin JL, Mouillet D, Nussbaum E, Ohnaka K, Pacheco J, Perrier C, Rabbia Y, Rebattu S, Reynaud F, Richichi A, Robini A, Sacchetti M, Schertl D, Schöller M, Solscheid W, Spang A, Stee P, Stefanini P, Tasso D, Testi L, von der Lühe O, Valtier JC, Vannier M and Ventura N (2007), Mar. Direct constraint on the distance of γ^2 Velorum from AMBER/VLTI observations. *A&A* 464 (1): 107–118. doi:10.1051/0004-6361:20065408. astro-ph/0610936.
- Milne EA (1926), May. On the possibility of the emission of high-speed atoms from the sun and stars. *MNRAS* 86: 459–473. doi:10.1093/mnras/86.7.459.
- Monnier JD, Tuthill PG and Danchi WC (1999), Nov. Pinwheel Nebula around WR 98A. *ApJ* 525 (2): L97–L100. doi:10.1086/312352. astro-ph/9909282.
- Monnier JD, Tuthill PG and Danchi WC (2002), Mar. Proper Motions of New Dust in the Colliding Wind Binary WR 140. *ApJ* 567 (2): L137–L140. doi:10.1086/340005. astro-ph/0202315.
- Monnier JD, Zhao M, Pedretti E, Millan-Gabet R, Berger JP, Traub W, Schloerb FP, ten Brummelaar T, McAlister H, Ridgway S, Sturm L, Sturmman J, Turner N, Baron F, Kraus S, Tannirkulam A and Williams PM (2011), Nov. First Visual Orbit for the Prototypical Colliding-wind Binary WR 140. *ApJ* 742 (1), L1. doi:10.1088/2041-8205/742/1/L1. 1111.1266.
- Moore T, Smartt SJ, Nicholl M, Srivastav S, Stevance HF, Jess DB, Grant SDT, Fulton MD, Rhodes L, Sim SA, Hirai R, Podsiadlowski P, Anderson JP, Ashall C, Bate W, Fender R, Gutiérrez CP, Howell DA, Huber ME, Inserra C, Leloudas G, Monard LAG, Müller-Bravo TE, Shappee BJ, Smith KW, Terreran G, Tony J, Tucker MA, Young DR, Aamer A, Chen TW, Ragosta F, Galbany L, Gromadzki M, Harvey L, Hoefflich P, McCully C, Newsome M, Gonzalez EP, Pellegrino C, Ramsden P, Pérez-Torres M, Ridley EJ, Sheng X and Weston J (2023), Oct. SN 2022jli: A Type Ic Supernova with Periodic Modulation of Its Light Curve and an Unusually Long Rise. *ApJ* 956 (1), L31. doi:10.3847/2041-8213/acfc25. 2309.12750.
- Motte F, Bontemps S and Louvet F (2018), Sep. High-Mass Star and Massive Cluster Formation in the Milky Way. *ARA&A* 56: 41–82. doi:10.1146/annurev-astro-091916-055235. 1706.00118.
- Nicholl M, Berger E, Smartt SJ, Margutti R, Kamble A, Alexander KD, Chen TW, Inserra C, Arcavi I, Blanchard PK, Cartier R, Chambers KC, Childress MJ, Chornock R, Cowperthwaite PS, Drout M, Flewelling HA, Fraser M, Gal-Yam A, Galbany L, Harmanen J, Holoién TWS, Hosseinzadeh G, Howell DA, Huber ME, Jerkstrand A, Kankare E, Kochanek CS, Lin ZY, Lunnan R, Magnier EA, Maguire K, McCully C, McDonald M, Metzger BD, Milisavljevic D, Mitra A, Reynolds T, Saario J, Shappee BJ, Smith KW, Valenti S, Villar VA, Waters C and Young DR (2016), Jul. SN 2015BN: A Detailed Multi-wavelength View of a Nearby Superluminous Supernova. *ApJ* 826 (1), 39. doi:10.3847/0004-637X/826/1/39. 1603.04748.
- North JR, Tuthill PG, Tango WJ and Davis J (2007), May. γ^2 Velorum: orbital solution and fundamental parameter determination with SUSI. *MNRAS* 377 (1): 415–424. doi:10.1111/j.1365-2966.2007.11608.x. astro-ph/0702375.
- Offner SSR, Moe M, Kratter KM, Sadavoy SI, Jensen ELN and Tobin JJ (2023), Jul., The Origin and Evolution of Multiple Star Systems, Inutsuka S, Aikawa Y, Muto T, Tomida K and Tamura M, (Eds.), *Protostars and Planets VII*, Astronomical Society of the Pacific Conference Series, 534, pp. 275, 2203.10066.
- Olivier GM, Lopez LA, Auchettl K, Rosen AL, Batta A, Neugent KF, Ramirez-Ruiz E, Jayasinghe T, Vallely PJ and Rowan DM (2022), Dec. A Multiwavelength Study of the Massive Colliding Wind Binary WR 20a: A Possible Progenitor for Fast-Spinning LIGO Binary Black Hole Mergers. *arXiv e-prints*, arXiv:2212.02514doi:10.48550/arXiv.2212.02514. 2212.02514.
- Paczyński B (1967), Jan. Evolution of Close Binaries. V. The Evolution of Massive Binaries and the Formation of the Wolf-Rayet Stars. *Acta Astron.* 17: 355.
- Parkin ER and Pittard JM (2008), Aug. A 3D dynamical model of the colliding winds in binary systems. *MNRAS* 388 (3): 1047–1061. doi:10.1111/j.1365-2966.2008.13511.x. 0805.4529.

- Peatt MJ, Richardson ND, Williams PM, Karnath N, Shenavrin VI, Lau RM, Moffat AFJ and Weigelt G (2023), Oct. FORCASTing the Spectroscopic Dust Properties of the WC+O Binary WR 137 with SOFIA. *ApJ* 956 (2), 109. doi:10.3847/1538-4357/acf201. 2308. 11798.
- Pellegrino C, Howell DA, Terreran G, Arcavi I, Bostroem KA, Brown PJ, Burke J, Dong Y, Gilkis A, Hiramatsu D, Hosseinzadeh G, McCully C, Modjaz M, Newsome M, Gonzalez EP, Pritchard TA, Sand DJ, Valenti S and Williamson M (2022), Oct. The Diverse Properties of Type Icn Supernovae Point to Multiple Progenitor Channels. *ApJ* 938 (1), 73. doi:10.3847/1538-4357/ac8ff6. 2205. 07894.
- Pittard JM and Dougherty SM (2006), Oct. Radio, X-ray, and γ -ray emission models of the colliding-wind binary WR140. *MNRAS* 372 (2): 801–826. doi:10.1111/j.1365-2966.2006.10888.x. astro-ph/0603787.
- Pittard JM, Dougherty SM, Coker RF, O'Connor E and Bolingbroke NJ (2006), Feb. Radio emission models of colliding-wind binary systems. Inclusion of IC cooling. *A&A* 446 (3): 1001–1019. doi:10.1051/0004-6361:20053649. astro-ph/0510283.
- Pittard JM, Vila GS and Romero GE (2020), Jun. Colliding-wind binary systems: diffusive shock acceleration and non-thermal emission. *MNRAS* 495 (2): 2205–2221. doi:10.1093/mnras/staa1099. 1912. 05299.
- Pledger JL, Sharp AJ and Sansom AE (2021), May. The detectability of Wolf-Rayet stars in M33-like spirals up to 30 Mpc. *MNRAS* 503 (2): 2168–2178. doi:10.1093/mnras/stab630. 2103. 01958.
- Pollock AMT, Corcoran MF, Stevens IR, Russell CMP, Hamaguchi K, Williams PM, Moffat AFJ, Weigelt G, Shenavrin V, Richardson ND, Espinoza D and Drake SA (2021), Dec. Competitive X-Ray and Optical Cooling in the Collisionless Shocks of WR 140. *ApJ* 923 (2), 191. doi:10.3847/1538-4357/ac2430. 2109. 10350.
- Prilutskii OF and Usov VV (1976), Feb. X rays from Wolf-Rayet binaries. *Soviet Ast.* 20: 2.
- Pshirkov MS (2016), Mar. The Fermi-LAT view of the colliding wind binaries. *MNRAS* 457 (1): L99–L102. doi:10.1093/mnras/1slv205. 1510. 03885.
- Rauw G and Nazé Y (2016), Sep. X-ray emission from interacting wind massive binaries: A review of 15 years of progress. *Advances in Space Research* 58 (5): 761–781. doi:10.1016/j.asr.2015.09.026. 1509. 06480.
- Rauw G, Crowther PA, De Becker M, Gosset E, Nazé Y, Sana H, van der Hucht KA, Vreux JM and Williams PM (2005), Mar. The spectrum of the very massive binary system WR 20a (WN6ha + WN6ha): Fundamental parameters and wind interactions. *A&A* 432 (3): 985–998. doi:10.1051/0004-6361:20042136.
- Reitberger K, Kissmann R, Reimer A, Reimer O and Dubus G (2014), Feb. High-energy Particle Transport in Three-dimensional Hydrodynamic Models of Colliding-wind Binaries. *ApJ* 782 (2), 96. doi:10.1088/0004-637X/782/2/96. 1401. 1323.
- Reitberger K, Reimer A, Reimer O and Takahashi H (2015), May. The first full orbit of η Carinae seen by Fermi. *A&A* 577, A100. doi:10.1051/0004-6361/201525726. 1503. 07637.
- Richardson ND, Shenar T, Roy-Loubier O, Schaefer G, Moffat AFJ, St-Louis N, Gies DR, Farrington C, Hill GM, Williams PM, Gordon K, Pablo H and Ramiamananantsoa T (2016), Oct. The CHARA Array resolves the long-period Wolf-Rayet binaries WR 137 and WR 138. *MNRAS* 461 (4): 4115–4124. doi:10.1093/mnras/stw1585. 1606. 09586.
- Richardson ND, Daly AR, Williams PM, Hill GM, Shenavrin VI, Endo I, Chené AN, Karnath N, Lau RM, Moffat AFJ and Weigelt G (2024), May. The long-period spectroscopic orbit and dust creation in the Wolf-Rayet binary system WR 125. *arXiv e-prints*, arXiv:2405.10454doi: 10.48550/arXiv.2405.10454. 2405. 10454.
- Roche PF and Aitken DK (1984), Jun. An investigation of the interstellar extinction. I. Towards dusty WC Wolf-Rayet stars. *MNRAS* 208: 481–492. doi:10.1093/mnras/208.3.481.
- Rodríguez LF, Arthur J, Montes G, Carrasco-González C and Toalá JA (2020), Sep. A Radio Pinwheel Emanating from WR 147. *ApJ* 900 (1), L3. doi:10.3847/2041-8213/abad9d. 2008. 03725.
- Ryder SD, Sadler EM, Subrahmanyan R, Weiler KW, Panagia N and Stockdale C (2004), Apr. Modulations in the radio light curve of the Type IIb supernova 2001ig: evidence for a Wolf-Rayet binary progenitor? *MNRAS* 349 (3): 1093–1100. doi:10.1111/j.1365-2966.2004.07589.x. astro-ph/0401135.
- Salas P, Bauer FE, Stockdale C and Prieto JL (2013), Jan. SN 2007bg: the complex circumstellar medium around one of the most radio-luminous broad-lined Type Ic supernovae. *MNRAS* 428 (2): 1207–1217. doi:10.1093/mnras/sts104. 1208. 3455.
- Salpeter EE (1952), Mar. Nuclear Reactions in Stars Without Hydrogen. *ApJ* 115: 326–328. doi:10.1086/145546.
- Sana H (2017), Nov., The multiplicity of massive stars: a 2016 view, Eldridge JJ, Bray JC, McClelland LAS and Xiao L, (Eds.), *The Lives and Death-Throes of Massive Stars*, 329, 110–117, 1703. 01608.
- Sana H and Evans CJ (2011), Jul., The multiplicity of massive stars, Neiner C, Wade G, Meynet G and Peters G, (Eds.), *Active OB Stars: Structure, Evolution, Mass Loss, and Critical Limits*, 272, 474–485, 1009. 4197.
- Sander AAC and Vink JS (2020), Nov. On the nature of massive helium star winds and Wolf-Rayet-type mass-loss. *MNRAS* 499 (1): 873–892. doi:10.1093/mnras/staa2712. 2009. 01849.
- Schönberner D, Balick B and Jacob R (2018), Feb. Expansion patterns and parallaxes for planetary nebulae. *A&A* 609, A126. doi:10.1051/0004-6361/201731788.
- Schootemeijer A, Shenar T, Langer N, Grin N, Sana H, Schürmann GGC, Wang C and Xu XT (2024), Jun. An absence of binary companions to Wolf-Rayet stars in the Small Magellanic Cloud: implications for mass loss and black hole masses at low metallicity. *arXiv e-prints*, arXiv:2406.01420doi:10.48550/arXiv.2406.01420. 2406. 01420.
- Seaquist ER (1976), Jan. Radio emission from the Wolf-Rayet binary gamma² Velorum. *ApJ* 203: L35–L37. doi:10.1086/182013.
- Shara MM, Howell SB, Furlan E, Gnlika CL, Moffat AFJ, Scott NJ and Zurek D (2022), Jan. A speckle-imaging search for close and very faint companions to the nearest and brightest Wolf-Rayet stars. *MNRAS* 509 (2): 2897–2907. doi:10.1093/mnras/stab2666. 2109. 06975.
- Shenar T (2024), Oct. Wolf-Rayet stars. *arXiv e-prints*, arXiv:2410.04436doi:10.48550/arXiv.2410.04436. 2410. 04436.
- Shenar T, Hamann WR and Todt H (2014), Feb. The impact of rotation on the line profiles of Wolf-Rayet stars. *A&A* 562, A118. doi:10.1051/0004-6361/201322496. 1401. 2159.
- Shenar T, Richardson ND, Sablowski DP, Hainich R, Sana H, Moffat AFJ, Todt H, Hamann WR, Oskinova LM, Sander A, Trammer F, Langer N, Bonanos AZ, de Mink SE, Gräfener G, Crowther PA, Vink JS, Almeida LA, de Koter A, Barbá R, Herrero A and Ulaczyk K (2017), Feb. The Tarantula Massive Binary Monitoring. II. First SB2 orbital and spectroscopic analysis for the Wolf-Rayet binary R145. *A&A* 598, A85. doi:10.1051/0004-6361/201629621. 1610. 07614.
- Shenar T, Gilkis A, Vink JS, Sana H and Sander AAC (2020), Feb. Why binary interaction does not necessarily dominate the formation of Wolf-Rayet stars at low metallicity. *A&A* 634, A79. doi:10.1051/0004-6361/201936948. 2001. 04476.
- Siebert MR, Decoursey C, Coulter DA, Engesser M, Piel JDR, Rest A, Egami E, Shahbandeh M, Chen W, Fox OD, Zenati Y, Moriya TJ, Bunker AJ, Cargile PA, Curti M, Eisenstein DJ, Gezari S, Gomez S, Guolo M, Johnson BD, Joshi BA, Karmen M, Maiolino R, Quimby RM, Robertson B, Strolger LG, Sun F, Wang Q and Wevers T (2024), Jun. Discovery of a Relativistic Stripped Envelope Type Ic-BL Supernova at $z = 2.83$ with JWST. *arXiv e-prints*, arXiv:2406.05076doi:10.48550/arXiv.2406.05076. 2406. 05076.
- Smartt SJ (2009), Sep. Progenitors of Core-Collapse Supernovae. *ARA&A* 47 (1): 63–106. doi:10.1146/annurev-astro-082708-101737. 0908. 0700.
- Smith N and Conti PS (2008), Jun. On the Role of the WNH Phase in the Evolution of Very Massive Stars: Enabling the LBV Instability with Feedback. *ApJ* 679 (2): 1467–1477. doi:10.1086/586885. 0802. 1742.

- Soulain A, Millour F, Lopez B, Matter A, Lagadec E, Carbillet M, La Camera A, Lamberts A, Langlois M, Milli J, Avenhaus H, Magnard Y, Roux A, Moulin T, Carle M, Sevin A, Martinez P, Abe L and Ramos J (2018), Oct. SPHERE view of Wolf-Rayet 104. Direct detection of the Pinwheel and the link with the nearby star. *A&A* 618, A108. doi:10.1051/0004-6361/201832817. 1806.08525.
- Soulain A, Lamberts A, Millour F, Tuthill P and Lau RM (2023), Jan. Smoke on the wind: dust nucleation in the archetype colliding-wind pinwheel WR 104. *MNRAS* 518 (3): 3211–3221. doi:10.1093/mnras/stac2999. 2209.01884.
- St-Louis N, Piaulet C, Richardson ND, Shenar T, Moffat AFJ, Eversberg T, Hill GM, Gauza B, Knapen JH, Kubát J, Kubátová B, Sablowski DP, Simón-Díaz S, Bolduan F, Dias FM, Dubreuil P, Fuchs D, Garrel T, Grutzeck G, Hunger T, Küsters D, Langenbrink M, Leadbeater R, Li D, Lopez A, Maucalire B, Moldenhawer T, Potter M, dos Santos EM, Schanne L, Schmidt J, Sieske H, Strachan J, Stinner E, Stinner P, Stober B, Strandbaek K, Syder T, Verilhac D, Waldschläger U, Weiss D and Wendt A (2020), Oct. An extensive spectroscopic time series of three Wolf-Rayet stars - II. A search for wind asymmetries in the dust-forming WC7 binary WR137. *MNRAS* 497 (4): 4448–4458. doi:10.1093/mnras/staa2214. 2007.09239.
- Stevens IR, Blondin JM and Pollock AMT (1992), Feb. Colliding Winds from Early-Type Stars in Binary Systems. *ApJ* 386: 265. doi:10.1086/171013.
- Stevens IR, Skinner SL, Nagase F, Corcoran MF, Willis AJ, Pollock AMT and Koyama K (1995), Feb. ASCA Observations of Colliding Stellar Winds in Gamma Velorum. *Ap&SS* 224 (1-2): 569–570. doi:10.1007/BF00667959.
- Tan JC, Beltrán MT, Caselli P, Fontani F, Fuente A, Krumholz MR, McKee CF and Stolte A (2014), Jan., Massive Star Formation, Beuther H, Klessen RS, Dullemond CP and Henning T, (Eds.), *Protostars and Planets VI*, 149–172, 1402.0919.
- Tolstoy E, Hill V and Tosi M (2009), Sep. Star-Formation Histories, Abundances, and Kinematics of Dwarf Galaxies in the Local Group. *ARA&A* 47 (1): 371–425. doi:10.1146/annurev-astro-082708-101650. 0904.4505.
- Tuthill PG, Monnier JD and Danchi WC (1999), Apr. A dusty pinwheel nebula around the massive star WR104. *Nature* 398 (6727): 487–489. doi:10.1038/19033. astro-ph/9904092.
- Tuthill PG, Monnier JD, Danchi WC, Wishnow EH and Haniff CA (2000), Apr. Michelson Interferometry with the Keck I Telescope. *PASP* 112 (770): 555–565. doi:10.1086/316550. astro-ph/0003146.
- Tuthill P, Monnier J, Tanner A, Figer D, Ghez A and Danchi W (2006), Aug. Pinwheels in the Quintuplet Cluster. *Science* 313: 935. doi:10.1126/science.1128731. astro-ph/0608427.
- Tuthill PG, Monnier JD, Lawrance N, Danchi WC, Owocki SP and Gayley KG (2008), Mar. The Prototype Colliding-Wind Pinwheel WR 104. *ApJ* 675 (1): 698–710. doi:10.1086/527286. 0712.2111.
- Ud-Doula A, Owocki SP and Townsend RHD (2009), Jan. Dynamical simulations of magnetically channelled line-driven stellar winds - III. Angular momentum loss and rotational spin-down. *MNRAS* 392 (3): 1022–1033. doi:10.1111/j.1365-2966.2008.14134.x. 0810.4247.
- Usov VV (1991), Sep. Stellar wind collision and dust formation in long-period, heavily interacting Wolf-Rayet binaries. *MNRAS* 252: 49. doi:10.1093/mnras/252.1.49.
- van Dalen JND, Levan AJ, Jonker PG, Malesani DB, Izzo L, Sarin N, Quirola-Vásquez J, Mata Sánchez D, de Ugarte Postigo A, van Hoof APC, Torres MAP, Schulze S, Littlefair SP, Chrimes A, Ravasio ME, Bauer FE, Martin-Carrillo A, Fraser M, van der Horst AJ, Jakobsson P, O'Brien P, De Pasquale M, Pugliese G, Sollerman J, Tanvir NR, Zafar T, Anderson JP, Galbany L, Gal-Yam A, Gromadzki M, Muller-Bravo TE, Ragosta F and Terwel JH (2024), Sep. The Einstein Probe transient EP240414a: Linking Fast X-ray Transients, Gamma-ray Bursts and Luminous Fast Blue Optical Transients. *arXiv e-prints*, arXiv:2409.19056doi:10.48550/arXiv.2409.19056. 2409.19056.
- van den Bergh S (1965), Aug. Light Echoes from Ancient Supernovae. *PASP* 77 (457): 269. doi:10.1086/128214.
- van der Hucht KA (2001), Feb. The VIIIth catalogue of galactic Wolf-Rayet stars. *New A Rev.* 45 (3): 135–232. doi:10.1016/S1387-6473(00)00112-3.
- van der Hucht KA, Morris PW, Williams PM, Setia Gunawan DYA, Beintema DA, Boxhoorn DR, de Graauw T, Heras A, Kester DJM, Lahuis F, Leech KJ, Roelfsema PR, Salama A, Valentijn EA and Vandebussche B (1996), Nov. ISO-SWS spectrophotometry of galactic Wolf-Rayet stars: preliminary results. *A&A* 315: L193–L196.
- Veen PM, van der Hucht KA, Williams PM, Catchpole RM, Duijsens MFJ, Glass IS and Setia Gunawan DYA (1998), Nov. A second dust episode of the Wolf-Rayet system WR 19: another long-period WC+O colliding-wind binary. *A&A* 339: L45–L48.
- Vink JS and de Koter A (2005), Nov. On the metallicity dependence of Wolf-Rayet winds. *A&A* 442 (2): 587–596. doi:10.1051/0004-6361:20052862. astro-ph/0507352.
- Vink JS and Harries TJ (2017), Jul. Wolf-Rayet spin at low metallicity and its implication for black hole formation channels. *A&A* 603, A120. doi:10.1051/0004-6361/201730503. 1703.09857.
- Vink JS, Gräfener G and Harries TJ (2011), Dec. In pursuit of gamma-ray burst progenitors: the identification of a sub-population of rotating Wolf-Rayet stars. *A&A* 536, L10. doi:10.1051/0004-6361/201118197. 1111.5806.
- Vrancken M, De Greve JP, Yungelson L and Tutukov A (1991), Sep. On the formation of WR+WR binaries. *A&A* 249: 411.
- Wallace DJ, Moffat AFJ and Shara MM (2002), Jan., Hubble Space Telescope Detection of Binary Companions Around Three WC9 Stars: WR 98a, WR 104, and WR 112, Moffat AFJ and St-Louis N, (Eds.), *Interacting Winds from Massive Stars*, Astronomical Society of the Pacific Conference Series, 260, pp. 407.
- Weiler KW, van Dyk SD, Panagia N, Sramek RA and Discenna JL (1991), Oct. The 10 Year Radio Light Curves for SN 1979C. *ApJ* 380: 161. doi:10.1086/170571.
- Weiler KW, van Dyk SD, Pringle JE and Panagia N (1992), Nov. Evidence for Periodic Modulation of Presupernova Mass Loss from the Progenitor of SN 1979C. *ApJ* 399: 672. doi:10.1086/171959.
- West SL, Lunnan R, Omand CMB, Kangas T, Schulze S, Strotjohann NL, Yang S, Fransson C, Sollerman J, Perley D, Yan L, Chen TW, Chen ZH, Taggart K, Fremling C, Bloom JS, Drake A, Graham MJ, Kasliwal MM, Laher R, Medford MS, Neill JD, Riddle R and Shupe D (2023), Feb. SN 2020qlb: A hydrogen-poor superluminous supernova with well-characterized light curve undulations. *A&A* 670, A7. doi:10.1051/0004-6361/202244086. 2205.11143.
- Williams PM (2019), Sep. Variable dust emission by WC type Wolf-Rayet stars observed in the NEOWISE-R survey. *MNRAS* 488 (1): 1282–1300. doi:10.1093/mnras/stz1784. 1906.11595.
- Williams PM, Beattie DH, Lee TJ, Stewart JM and Antonopoulou E (1978), Nov. Condensation of a shell around HD 193793. *MNRAS* 185: 467–472. doi:10.1093/mnras/185.3.467.
- Williams PM, van der Hucht KA and The PS (1987), Sep. Variable dust emission from Wolf-Rayet stars. *QJRAS* 28: 248–253.
- Williams PM, van der Hucht KA, Pollock AMT, Florkowski DR, van der Woerd H and Wamsteker WM (1990), Apr. Multi-frequency variations of the Wolf-rayet system HD 193793 - I. Infrared, X-ray and radio observations. *MNRAS* 243: 662–684.
- Williams PM, Dougherty SM, Davis RJ, van der Hucht KA, Bode MF and Setia Gunawan DYA (1997), Jul. Radio and infrared structure of the colliding-wind Wolf-Rayet system WR147. *MNRAS* 289 (1): 10–20. doi:10.1093/mnras/289.1.10.
- Williams PM, Marchenko SV, Marston AP, Moffat AFJ, Varricatt WP, Dougherty SM, Kidger MR, Morbidelli L and Tapia M (2009a), May. Orbitally modulated dust formation by the WC7+O5 colliding-wind binary WR140. *MNRAS* 395 (3): 1749–1767. doi:10.1111/j.1365-2966.2009.14664.x. 0902.4540.

- Williams PM, Rauw G and van der Hucht KA (2009b), Jun. Dust formation by the colliding wind WC5+O9 binary WR19 at periastron passage. *MNRAS* 395 (4): 2221–2225. doi:10.1111/j.1365-2966.2009.14681.x. 0902.4105.
- Williams PM, van der Hucht KA, van Wyk F, Marang F, Whitelock PA, Bouchet P and Setia Gunawan DYA (2012), Mar. Recurrent dust formation by WR 48a on a 30-year time-scale. *MNRAS* 420 (3): 2526–2538. doi:10.1111/j.1365-2966.2011.20218.x. 1111.5194.
- Williams PM, Varricatt WP, Chené AN, Corcoran MF, Gull TR, Hamaguchi K, Moffat AFJ, Pollock AMT, Richardson ND, Russell CMP, Sander AAC, Stevens IR and Weigelt G (2021), May. Conditions in the WR 140 wind-collision region revealed by the 1.083- μ m He I line profile. *MNRAS* 503 (1): 643–659. doi:10.1093/mnras/stab508. 2102.09445.
- Willis AJ (1982), Mar. P-Cyg profiles observed in the ultraviolet and visible spectra of Wolf-Rayet stars. *MNRAS* 198: 897–920. doi:10.1093/mnras/198.4.897.
- Wolf CJE and Rayet G (1867), Jan. Spectroscopie stellaire. *Academie des Sciences Paris Comptes Rendus* 65: 292–296.
- Woosley SE (1993), Mar. Gamma-Ray Bursts from Stellar Mass Accretion Disks around Black Holes. *ApJ* 405: 273. doi:10.1086/172359.
- Woosley SE and Bloom JS (2006), Sep. The Supernova Gamma-Ray Burst Connection. *ARA&A* 44 (1): 507–556. doi:10.1146/annurev.astro.43.072103.150558. astro-ph/0609142.
- Woosley SE and Heger A (2006), Feb. The Progenitor Stars of Gamma-Ray Bursts. *ApJ* 637 (2): 914–921. doi:10.1086/498500. astro-ph/0508175.
- Woosley SE, Heger A and Weaver TA (2002), Nov. The evolution and explosion of massive stars. *Reviews of Modern Physics* 74 (4): 1015–1071. doi:10.1103/RevModPhys.74.1015.
- Wright AE and Barlow MJ (1975), Jan. The radio and infrared spectrum of early type stars undergoing mass loss. *MNRAS* 170: 41–51. doi:10.1093/mnras/170.1.41.
- Zavala S, Toalá JA, Santamaría E, Ramos-Larios G, Sabin L, Quino-Mendoza JA, Rubio G and Guerrero MA (2022), Jul. 3D mapping of the Wolf-Rayet nebula M 1-67: clues for post-common envelope evolution in massive stars. *MNRAS* 513 (3): 3317–3325. doi:10.1093/mnras/stac1097. 2204.07778.
- Zhekov SA (2021), Jan. Colliding stellar wind modelling of the X-ray emission from WR 140. *MNRAS* 500 (4): 4837–4848. doi:10.1093/mnras/staa3591. 2011.08550.
- Zhekov SA and Park S (2010a), Sep. Chandra HETG Observations of the Colliding Stellar Wind System WR 147. *ApJ* 721 (1): 518–529. doi:10.1088/0004-637X/721/1/518. 1007.4352.
- Zhekov SA and Park S (2010b), Feb. Chandra Observations of WR 147 Reveal a Double X-ray Source. *ApJ* 709 (2): L119–L123. doi:10.1088/2041-8205/709/2/L119. 0912.3554.
- Zhekov SA, Tomov T, Gawronski MP, Georgiev LN, Borissova J, Kurtev R, Gagné M and Hajduk M (2014), Dec. A multiwavelength view on the dusty Wolf-Rayet star WR 48a*. *MNRAS* 445 (2): 1663–1678. doi:10.1093/mnras/stu1880. 1409.2684.
- Zhekov SA, Gagné M and Skinner SL (2022), Feb. Chandra revisits WR 48a: testing colliding wind models in massive binaries. *MNRAS* 510 (1): 1278–1288. doi:10.1093/mnras/stab3469. 2111.13515.